**Figure 2.** Ten isoforms of *TEL/PTPRR* cDNAs generated through alternative splicing. *A,* schematic structures of wild-type TEL and wild-type PTPRR. *Solid triangles,* breakpoints in each protein. *HLH,* helix-loop-helix oligomerization domain; *ETS,* ETS DNA-binding domain; *TM,* transmembrane domain; *PTP,* protein tyrosine phosphatase domain (catalytic domain). *B,* schematic presentation of 10 *TEL/PTPRR* isoforms. Exons surrounding the junctions are presented as boxes to emphasize exon skipping. *Solid triangles* and *arrows,* fusion points and locations of stop codon, respectively. *C,* nucleotide sequences and deduced amino acids around the breakpoints of the two dominant isoforms (tTEL and TEL/PTPRR). *D,* dominant amplification of *tTEL* and *TEL/PTPRR* in RT-PCR assay. A set of primers TELf1 (in *TEL* exon 1) and PTPRRr14 (in *PTPRR* exon 14) was used to amplify full-length *TEL/PTPRR* cDNA.
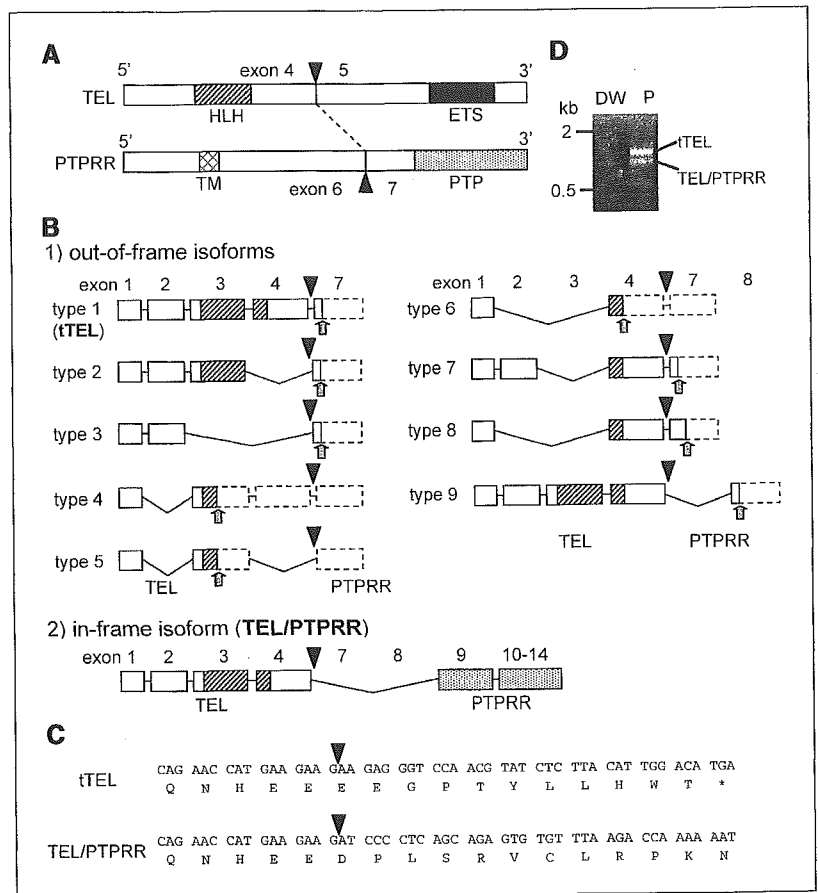
detected in spite of our efforts with several sets of primers including the one described above. Thus, we conclude that *TEL/PTPRR* is expressed in the leukemic cells of this patient and might therefore contribute to leukemogenesis. Wild-type *TEL* mRNA probably derived from the intact *TEL* allele was expressed in the leukemic cells, whereas wild-type *PTPRR* mRNA was not.

Alternative splicing leads to generation of 10 *TEL/PTPRR* chimeric cDNAs. Because the *TEL* gene was fused out-of-frame to the *PTPRR* gene, the resultant full-length *TEL/PTPRR* cDNA (type 1) represented an open reading frame encoding exons 1 to 4 of the *TEL* gene (154 amino acids) with additional 11 amino acids (Fig. 2*B* and *C*). This isoform expresses truncated TEL including the intact helix-loop-helix domain, but lacks the COOH-terminal ETS domain of TEL and any functional domains of PTPRR. We thus refer to it as "truncated TEL (tTEL)" in the following sections. To seek for other *TEL/PTPRR* isoforms in the inv(12)(p13q13)-carrying leukemic cells, we further did RT-PCR analysis with other combinations of primers. When we used a set of primers TELf1 (in *TEL* exon 1) and PTPRRr7b (in *PTPRR* exon 7), various *TEL/PTPRR* cDNAs of smaller sizes were amplified as well as a full-length cDNA (data not shown). Sequencing analysis showed that exon-skipping mechanisms in the *TEL* gene produced seven isoforms (types 2-8). All these isoforms were also out-of-frame and should express only the NH$_2$-terminal portion of TEL in which a part or the entire of the helix-loop-helix domain is spliced out. Moreover, using another set of primers TELf3 (in *TEL* exon 3) and PTPRRr10 (in *PTPRR* exon 10), we identified two other isoforms that lacked exon 7 (type 9) or exons 7 and 8 (TEL/PTPRR) of the

PTPRR gene. Although type 9 isoform again contained an out-of-frame junction, TEL/PTPRR was the unique in-frame isoform with an open reading frame of 1,158 nucleotides coding for 385 amino acid residues that linked the helix-loop-helix domain of TEL and almost the entire protein tyrosine phosphatase domain of PTPRR (Fig. 2*B* and *C*). RT-PCR with a combination of primers PTPRRf10 (in *PTPRR* exon 10) and PTPRRr14 (in *PTPRR* exon 14) amplified only one kind of cDNA that contained exons 10 to 14 of the *PTPRR* gene without any deletions (data not shown), indicating that alternative splicing did not occur in this region. To examine which of these 10 isoforms were dominantly expressed in the leukemic cells, we then made PCR amplification with a set of primers TELf1 and PTPRRr14. Interestingly, two major bands which turned out to be derived from *tTEL* and *TEL/PTPRR* by sequencing analysis were observed (Fig. 2*D*). Thus, we decided to investigate molecular and biological functions of these two isoforms in the following experiments to establish the underlying mechanisms in inv(12)-type leukemia.

Truncated TEL and TEL/PTPRR affect nuclear localization of wild-type TEL. We first induced wild-type TEL, tTEL, or TEL/PTPRR expression in COS-7 cells by transfecting the corresponding cDNAs into them. As previously reported (42), slow-migrating bands were detected in addition to that of the expected size, when wild-type TEL was expressed (Fig. 3*A, left*). tTEL and TEL/PTPRR proteins also showed similar slow-migrating bands. When these proteins were metabolically labeled with [^{32}P]orthophosphate, all these size-shifted bands for wild-type TEL, tTEL, or TEL/PTPRR turned out to be hyperphosphorylated forms (Fig. 3*A, right*). The lowest band of

−43−
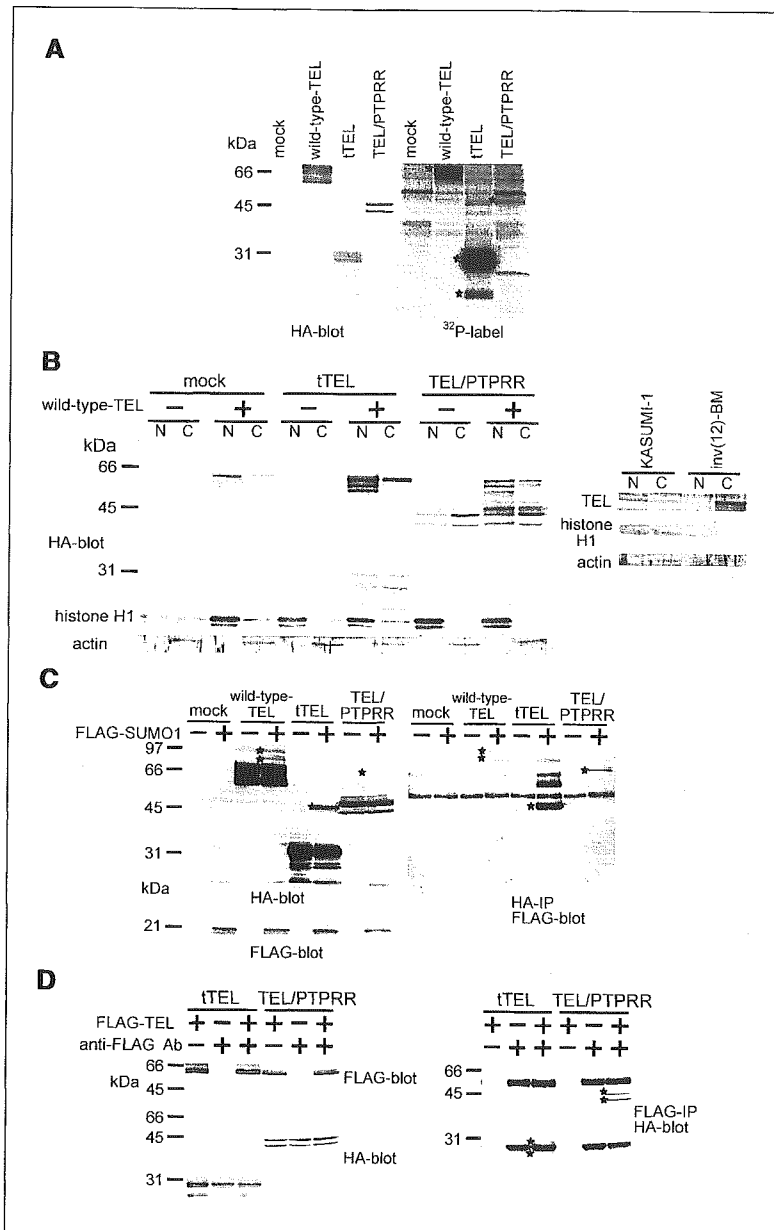
Figure 3. Subcellular localization, SUMO-1 modification, and heterodimerization with wild-type TEL of tTEL and TEL/PTPRR. A, truncated TEL and TEL/PTPRR are phosphorylated in vivo. Left, expression of hemagglutinin-tagged wild-type TEL, tTEL, and TEL/PTPRR in COS-7 cells was confirmed by Western blot analysis with anti-hemagglutinin antibody. Right, COS-7 cells expressing each protein were subjected to metabolic labeling with [^{32}P]orthophosphate. The lysates were immunoprecipitated with anti-hemagglutinin antibody. Asterisks, phosphorylated wild-type TEL, tTEL, and TEL/PTPRR. B, truncated TEL and TEL/PTPRR change subcellular localization of wild-type TEL. Left, hemagglutinin-tagged wild-type TEL, tTEL, and TEL/PTPRR were transiently expressed in NIH3T3 cells as indicated. Equal volumes of nuclear (N) or cytoplasmic (C) fraction were subjected to Western blot analysis with anti-hemagglutinin antibody. Right, non-inv(12)-carrying KASUMI-1 cells and inv(12)-carrying leukemic cells were also fractionated and subjected to Western blot analysis with anti-TEL antibody (N-19). Endogenous histone H1 and actin were immunoblotted as nuclear and cytoplasmic markers, respectively. C, both tTEL and TEL/PTPRR are sumoylated. Left, COS-7 cell lysates expressing hemagglutinin-tagged wild-type TEL, tTEL, or TEL/PTPRR, alone or along with FLAG-tagged SUMO-1, were immunoblotted with anti-hemagglutinin antibody. Asterisks, sumoylated wild-type TEL, tTEL, and TEL/PTPRR. Expression of FLAG-tagged SUMO-1 was confirmed by Western blot analysis with anti-FLAG antibody. Right, these lysates were subjected to immunoprecipitation with anti-hemagglutinin antibody, followed by Western blot analysis with anti-FLAG antibody. D, both tTEL and TEL/PTPRR associate with wild-type TEL in vivo. Left, COS-7 cell lysates expressing FLAG-tagged wild-type TEL, hemagglutinin-tagged tTEL or TEL/PTPRR, or both FLAG-tagged wild-type TEL and hemagglutinin-tagged tTEL or TEL/PTPRR were immunoblotted with anti-FLAG or anti-hemagglutinin antibody. Right, these lysates were subjected to immunoprecipitation with anti-FLAG antibody, followed by Western blot analysis with anti-hemagglutinin antibody. Asterisks, hemagglutinin-tagged TEL and TEL/PTPRR.

tTEL was likely to be derived from a degradation product. Given that Ser^{22} in wild-type TEL is a constitutive phosphorylation site (42), these aberrant TEL proteins could have been also phosphorylated at least on the same residue and showed larger-sized bands.

To get some insights into molecular functions of the aberrant TEL proteins, we next examined subcellular localization of tTEL and TEL/PTPRR by Western blot analysis with fractionated lysates overexpressing each protein. We confirmed that specific marker for nuclear or cytoplasmic fraction, histone H1 or actin, was exclusively located in the corresponding fraction (Fig. 3B, left). Because both tTEL and TEL/PTPRR lack ETS DNA-binding domain of TEL containing nuclear localization signal, and ETS-lacking mutant or isoforms of wild-type TEL have been reported to reside in the cytoplasm (41, 44), it is quite plausible that they show different distribution patterns from that of wild-type TEL. When wild-type TEL cDNA was transiently transfected to NIH3T3 cells, overexpressed wild-type TEL protein was predominantly localized

in the nucleus. On the other hand, overexpressed tTEL protein was exclusively distributed in the cytoplasm and overexpressed TEL/PTPRR chimeric protein also chiefly resided in the cytoplasm. Surprisingly, when tTEL or TEL/PTPRR was coexpressed with wild-type TEL, all these proteins were almost equally expressed in both fractions. These data suggest that both tTEL and TEL/PTPRR prevent de novo translated wild-type TEL from entering the nucleus, whereas wild-type TEL draws tTEL and TEL/PTPRR into the nucleus. We further compared subcellular localization of endogenous wild-type TEL between the inv(12)-carrying M2 leukemic cells and t(8;21)-carrying M2 KASUMI-1 cells. Interestingly, whereas endogenous TEL proteins were predominantly distributed to the nucleus in KASUMI-1 cells, they were exclusively cytoplasmic in the inv(12)-carrying cells (Fig. 3B, right).

It has been reported that wild-type TEL is sumoylated on Lys^{99} and that sumoylated wild-type TEL is a target of CRM1-mediated nuclear export (44, 45). Because tTEL and TEL/PTPRR

−44−

encompassed the acceptor site and mainly resided in the cytoplasm, we examined whether they were modified by SUMO-1. COS-7 cells were transfected with hemagglutinin-tagged wild-type TEL, tTEL, or TEL/PTPRR expression plasmid with or without FLAG-tagged SUMO-1 plasmid. As reported on wild-type TEL, bands corresponding to SUMO-1–modified proteins (wild-type TEL, 75 and 85 kDa; tTEL, 45 kDa; TEL/PTPRR, 65 kDa) were detected in Western blot analysis with anti-hemagglutinin antibody only when SUMO-1 plasmid was cotransfected (Fig. 3C, left). To confirm that these larger-sized bands were indeed derived from SUMO-1–modified proteins, the total cell lysates were immunoprecipitated with anti-hemagglutinin antibody. The precipitated proteins were visualized with anti-FLAG antibody at the expected sizes of each SUMO-1–conjugated protein (Fig. 3C, right). Therefore, we conclude that both tTEL and TEL/PTPRR are subjected to modification with SUMO-1, which may support their cytoplasmic localization. As an additional remark, several proteins of higher molecular weights than sumoylated tTEL were concomitantly immunoprecipitated with anti-hemagglutinin antibody in the presence of exogenous SUMO-1. Because they were not detected with anti-hemagglutinin antibody but with anti-FLAG antibody, a likely scenario is that some other SUMO-1–modified proteins interacting with tTEL were coimmunoprecipitated.

Truncated TEL and TEL/PTPRR heterodimerize with wild-type TEL. Because tTEL and TEL/PTPRR contain the entire helix-loop-helix domain of TEL, they conceivably heterodimerize with wild-type TEL. To test this hypothesis, we transiently transfected into COS-7 cells hemagglutinin-tagged tTEL or TEL/PTPRR expression plasmid, alone or along with FLAG-tagged wild-type TEL expression plasmid. Cell lysates were subjected to immunoprecipitation with anti-FLAG antibody followed by Western blot analysis with anti-hemagglutinin antibody. As shown in Fig. 3D, both tTEL and TEL/PTPRR were coimmunoprecipitated with anti-FLAG antibody when they were coexpressed with FLAG-tagged wild-type TEL. This coimmunoprecipitation completely disappeared when anti-FLAG antibody was removed from the reaction or when FLAG-tagged wild-type TEL was not coexpressed in COS-7 cells. Moreover, when we applied anti-hemagglutinin antibody for immunoprecipitation, FLAG-tagged wild-type TEL was coimmunoprecipitated with hemagglutinin-tagged tTEL or TEL/PTPRR (data not shown). These data indicate that these aberrant proteins heterodimerize with wild-type TEL *in vivo*.

TEL/PTPRR prevents wild-type TEL from binding to ETS-binding consensus site. Because the breakpoint occurs between exons 4 and 5 of the *TEL* gene, neither tTEL nor TEL/PTPRR encodes the ETS domain of TEL. It is therefore quite likely that these isoforms do not possess EBS-specific DNA-binding property as wild-type TEL does. To clarify this point, wheat germ extracts expressing wild-type TEL, tTEL, and TEL/PTPRR at comparable levels (Fig. 4A) were applied to EMSA in which radioactive EBS

Figure 4. Truncated TEL and TEL/PTPRR confer a dominant-negative effect over wild-type TEL. *A,* expression of hemagglutinin-tagged wild-type TEL, tTEL, or TEL/PTPRR in the lysates prepared by *in vitro* translation system. Western blot analysis was done with anti-hemagglutinin antibody. *B,* EMSA with the lysates and ^{32}P-labeled EBS probe. *Left,* both tTEL and TEL/PTPRR lack EBS-specific DNA-binding ability. In competition assay, a 300-fold molar excess of specific competitor (*S.C.*) or nonspecific competitor (*N.C.*) was added to the reaction mixtures. *Arrowhead,* broad band derived from EBS-TEL complex. In supershift assay, anti-TEL (N-19) antibody was added to the reaction mixtures. *Arrow,* supershifted band. *Right,* TEL/PTPRR inhibits wild-type TEL from binding to EBS. *In vitro* translated lysates were mixed as indicated. *Lanes 2* to *4,* the amount of wild-type TEL lysates was kept constant. *Asterisks,* EBS-TEL complex. *C,* luciferase reporter assays. *Top,* HeLa cells were transfected with 1 μg of (EBS)$_3$tkLuc reporter plasmid, alone or along with increasing amounts (0.1, 0.5, and 1.0 μg) of the indicated expression plasmids. *Bottom,* HeLa cells were transfected with 1 μg of (EBS)$_3$tkLuc, alone or along with 0.1 μg of wild-type TEL expression plasmid. Increasing amounts (0.05, 0.5, and 0.9 μg) of tTEL or TEL/PTPRR expression plasmid was also added. To emphasize transcriptional repression, reciprocals of relative luciferase activities presenting average results of duplicate experiments are shown as "fold repression." *D,* aberrant TEL proteins relieve suppressed expression of endogenous Bcl-X$_L$ mediated by wild-type TEL. NIH3T3 cells retrovirally infected with empty or FLAG-tagged wild-type TEL vector were transiently transfected with tTEL or TEL/PTPRR expression plasmid. *Top,* cell lysates were subjected to Western blot analysis with anti-Bcl-X$_L$ antibody. *Middle* and *bottom,* constitutive expression of FLAG-tagged wild-type TEL and transient expression of hemagglutinin-tagged tTEL and TEL/PTPRR were confirmed by Western blot analysis with anti-FLAG and anti-hemagglutinin antibodies, respectively.

−45−
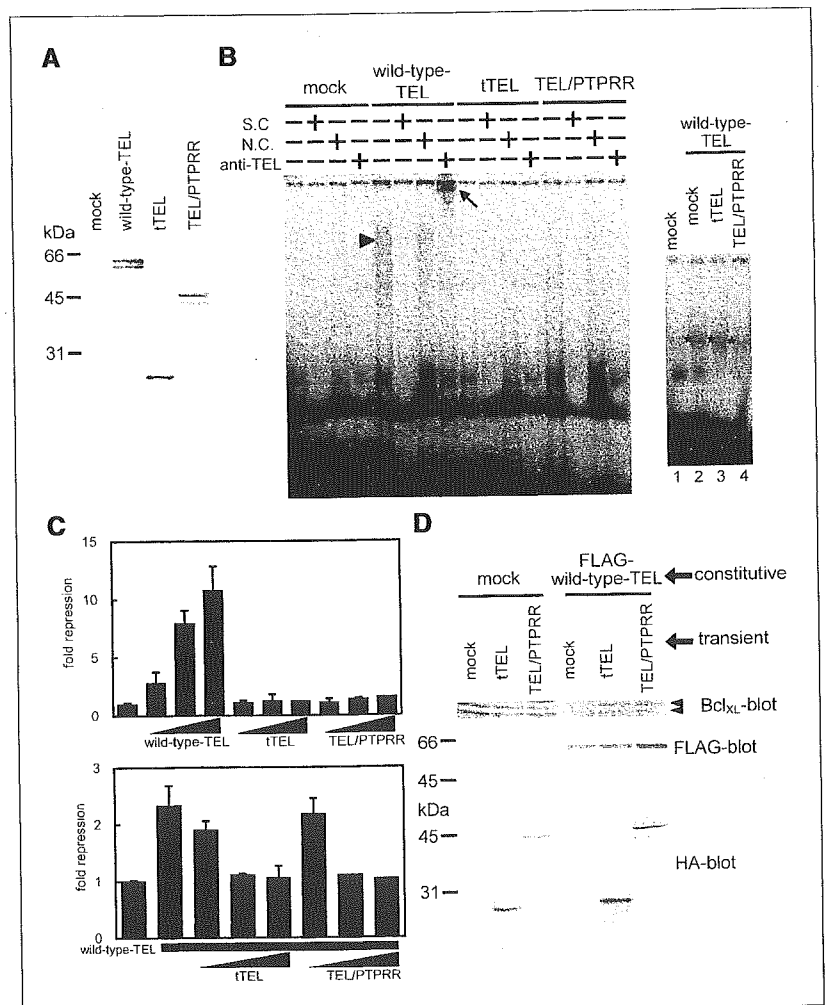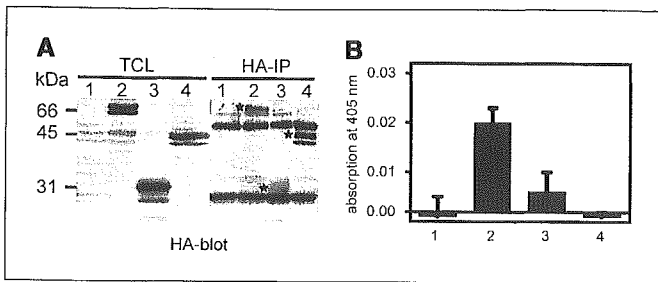
Figure 5. Truncated TEL and TEL/PTPRR lack phosphatase activity. *A,* expression and immunoprecipitation of hemagglutinin-tagged wild-type PTPRR, tTEL, or TEL/PTPRR in COS-7 cell lysates. Western blot analysis was done with anti-hemagglutinin antibody. *Lane 1,* mock; *lane 2,* wild-type PTPRR; *lane 3,* tTEL; *lane 4,* TEL/PTPRR. *B, in vitro* phosphatase assay using *p*-nitrophenyl phosphate as a substrate. Nonenzymatic hydrolysis of *p*-nitrophenyl phosphate was subtracted from the measured values. *Columns,* averages of duplicate experiments.

oligonucleotide was used as a probe. As previously observed (2, 40), wild-type TEL formed a specific DNA-protein complex that emerged as a somewhat broad band possibly due to weak binding (Fig. 4B, left). This band represented a specific association of wild-type TEL and the EBS probe because it was completely canceled by cold specific competitor but not by nonspecific competitor. Furthermore, this band was supershifted when anti-TEL antibody was preincubated with the lysate. In contrast, neither tTEL nor TEL/PTPRR formed a specific DNA-protein compound. Taken together, we conclude that both isoforms lose EBS-specific DNA-binding capacity.

We next examined whether tTEL and TEL/PTPRR alter the capacity of wild-type TEL to bind with EBS. Whereas mixture of

wild-type TEL and tTEL did not change the intensity of the band derived from possible EBS-TEL complex, mixture of wild-type TEL and TEL/PTPRR obviously diminished it (Fig. 4B, right). We confirmed that the shifted bands contained wild-type TEL protein by the supershift experiment with anti–COOH-terminal TEL antibody (data not shown). This result indicates that TEL/PTPRR prevents wild-type TEL molecule from binding to EBS, possibly by heterodimerizing with it.

Truncated TEL and TEL/PTPRR themselves do not repress transcription through ETS-binding consensus site, but confer a dominant-negative effect over wild-type TEL. TEL is a member of ETS family transcription factors and represses transcription of target genes through EBS. Because both tTEL and TEL/PTPRR lack the ETS domain and thus do not bind to EBS, they could lose activity as a transcription factor. We thus did luciferase reporter assays with (EBS)$_3$tkLuc and examined the effects of tTEL and TEL/PTPRR on transcription through EBS in HeLa cells. When increasing amounts of wild-type TEL expression plasmid were cotransfected with (EBS)$_3$tkLuc, the luciferase activities were repressed in a dose-dependent manner (Fig. 4C, top). This transcriptional regulation was EBS specific because no repression was observed when (EBS)$_3$tkLuc was substituted with a mutant reporter plasmid, (mEBS)$_3$tkLuc (data not shown). On the other hand, transfection of tTEL or TEL/PTPRR expression plasmid along with (EBS)$_3$tkLuc yielded no significant changes in luciferase activities even at the highest dose.

Because they were found to associate with wild-type TEL, we then speculated that tTEL and TEL/PTPRR could affect the functions of wild-type TEL by heterodimerizing with it. Thus, increasing amounts of tTEL or TEL/PTPRR expression plasmid were transfected with (EBS)$_3$tkLuc and wild-type TEL expression plasmid.
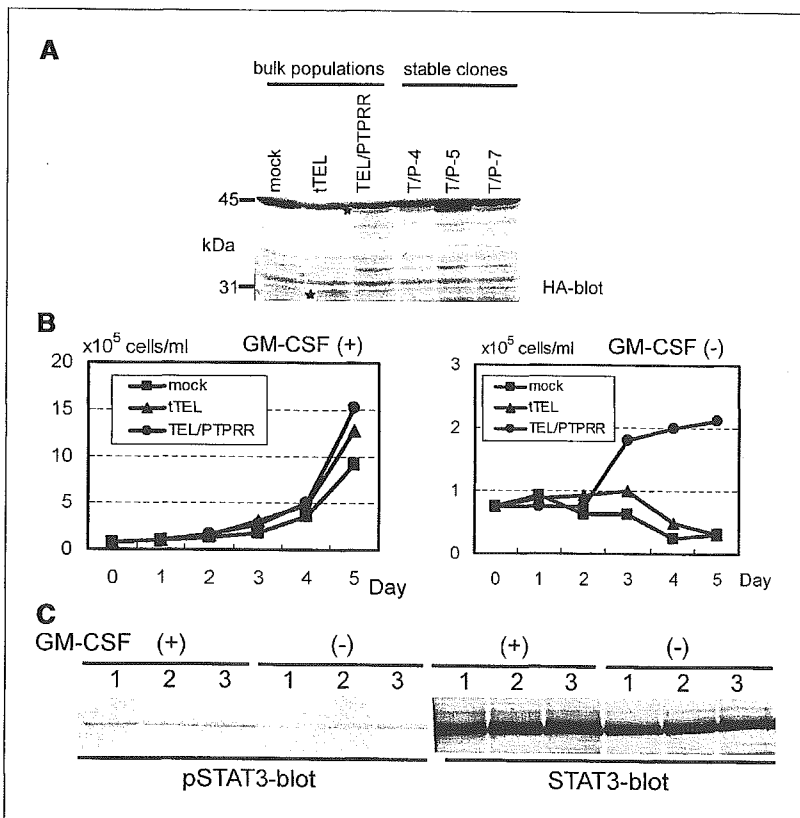
Figure 6. TEL/PTPRR renders UT7/GM cells factor independent. *A,* expression of tTEL and TEL/PTPRR in the bulk and stable populations of UT7/GM cells. These cells were obtained by electroporating the corresponding expression plasmids and selecting cells by G418 resistance. Western blot analysis was done with anti-hemagglutinin antibody. *Asterisks,* overexpressed proteins. *B,* UT7/GM cells overexpressing TEL/ PTPRR show GM-CSF–independent proliferation. UT7/GM cells expressing the indicated proteins were cultured in the presence (*left*) or absence (*right*) of GM-CSF. Cells were suspended in culture media at a concentration of 0.8 × 10⁵ cells/mL at day 0, and cell numbers were counted at the indicated time points. *C,* phosphorylated STAT3 is retained after factor withdrawal in tTEL- and TEL/PTPRR-overexpressing UT7/GM cells. Cells were cultured in the presence or absence of GM-CSF for 96 hours before the harvest. Lysates were immunoprecipitated with anti-STAT3 antibody and applied to Western blot analysis with anti–phosphorylated STAT3 (*left*) or anti-STAT3 (*right*) antibody. *Lane 1,* mock; *lane 2,* tTEL; *lane 3,* TEL/PTPRR.

-46-

Interestingly, this led to a decrease in fold repression induced by wild-type TEL (Fig. 4*C, bottom*). These data suggest that both tTEL and TEL/PTPRR exert a dominant-negative effect on wild-type TEL–mediated transcriptional repression and that tumor-suppressive functions of wild-type TEL may be abolished in the leukemic cells.

To confirm the dominant-negative effect of tTEL and TEL/PTPRR over wild-type TEL *in vivo*, we evaluated by Western blot analysis the endogenous expression of *Bcl-X$_L$*, a well-known transcriptional target of TEL. For this purpose, NIH3T3 cells constitutively expressing FLAG-tagged wild-type TEL were transiently transfected with tTEL or TEL/PTPRR expression plasmid, and were subjected to Western blot analysis with anti–Bcl-X$_L$ antibody. As previously reported (11), expression of endogenous Bcl-X$_L$ was found repressed by wild-type TEL (Fig. 4*D*). Importantly, coexpression of tTEL and TEL/PTPRR recovered suppressed Bcl-X$_L$ expression in the wild-type TEL–expressing cells.

TEL/PTPRR lacks protein tyrosine phosphatase activity. PTPRR, a human homologue of PTPSL/PTPBr7 in mouse and PC12-PTP1/PCPTP1 in rat, is a receptor-type tyrosine phosphatase that contains one cytoplasmic protein tyrosine phosphatase domain at its COOH terminus. Because TEL/PTPRR possesses almost full length of the protein tyrosine phosphatase domain, we analyzed if it retained catalytic activity by *in vitro* phosphatase assay using *p*-nitrophenyl phosphate as a substrate. Lysates from COS-7 cells overexpressing hemagglutinin-tagged wild-type PTPRR, tTEL, or TEL/PTPRR were immunoprecipitated with anti-hemagglutinin antibody. To confirm that each protein was successfully collected, a portion of immunoprecipitates and total cell lysates was subjected to Western blot analysis (Fig. 5*A*). All these proteins were gathered at comparable levels. Wild-type PTPRR showed catalytic activity as a protein tyrosine phosphatase (Fig. 5*B*). In contrast, tTEL completely lacking the protein tyrosine phosphatase domain was catalytically inactive, as expected. Surprisingly enough, TEL/PTPRR also lost its activity, probably because it did not express the 13 NH$_2$-terminal amino acid residues of the protein tyrosine phosphatase domain. We speculate that phosphatase activity is not a requisite for the development of inv(12)-carrying leukemia.

TEL/PTPRR endows UT7/GM cells with factor independence. To search for transforming activity of tTEL and TEL/PTPRR, we employed the human megakaryocytic leukemia cell line UT7/GM that requires GM-CSF for proliferation and survival, and analyzed the effects of overexpressed tTEL or TEL/PTPRR on the factor-dependent growth. By using electroporation, we introduced tTEL or TEL/PTPRR expression plasmid into UT7/GM cells. As indicated in Fig. 6*A*, Western blot analysis with anti-hemagglutinin antibody showed the comparable expression of tTEL and TEL/PTPRR proteins in the bulk populations and we used these uncloned cells in the following experiments. When cultured under the presence of GM-CSF, both tTEL- and TEL/PTPRR-overexpressing cells proliferated slightly faster than mock cells (Fig. 6*B*). Mock cells expectedly starved to death after depletion of GM-CSF from the media. The tTEL-overexpressing cells did not survive after cytokine removal either. In contrast, the TEL/PTPRR-overexpressing cells continued to proliferate slowly in factor-free media at least beyond day 60 of culture. We also established by limiting dilution three stable lines overexpressing TEL/PTPRR (T/P-4, T/P-5, and T/P-7), and confirmed the factor independence beyond 2 months of culture. The calculated doubling times at day 28 were 45, 34, and 76 hours, respectively. These observations suggest that the GM-

CSF–independent survival is not due to selection and expansion of mutated clones, but results from the expression of TEL/PTPRR itself.

We hypothesized that some growth signalings were constitutively activated in the TEL/PTPRR-overexpressing cells, leading to the factor-independent proliferation. To identify the exaggerated signals in these cells, we next compared the phosphorylation levels of molecules in various signal transduction systems including mitogen-activated protein (MAP) kinase signals, JAK/STAT signals, and phosphatidylinositol 3-kinase signals among mock, tTEL-, and TEL/PTPRR-overexpressing cells. We observed that c-jun-NH$_2$-kinase (JNK) in the MAP kinase signalings, STAT1 and STAT5 in the JAK/STAT signalings, and Akt1/2/3 in the phosphatidylinositol 3-kinase signalings were almost equally phosphorylated among them and their phosphorylation levels remained unchanged before and after the cytokine removal (data not shown). Extracellular signal-regulated kinase (ERK)-1/2 in the MAP kinase signalings alone became almost thoroughly dephosphorylated within 12 hours after the factor deprivation in all the bulk populations. On the other hand, in spite of the steady expression of STAT3 proteins, phosphorylated STAT3 rapidly declined after GM-CSF withdrawal in the mock cells (Fig. 6*C*). Notably, however, the levels of phosphorylated STAT3 were unaltered in the tTEL- and TEL/PTPRR-overexpressing cells. These data suggest that overexpressed mutant TEL proteins, tTEL and TEL/PTPRR, might stimulate the JAK/STAT signal via STAT3, but that TEL/PTPRR might activate other pathways to render UT7/GM cells factor independent.

Discussion

We have shown in this study that inv(12)(p13q13) results in the formation of the *TEL/PTPRR* chimeric gene, fusing exon 4 in the *TEL* gene with exon 7 in the *PTPRR* gene. Ten isoforms of the *TEL/PTPRR* cDNAs that are generated possibly through alternative splicing have been cloned in RT-PCR assay. Among the isoforms, only one isoform encodes a chimeric product (TEL/PTPRR) connecting the helix-loop-helix domain of TEL and the protein tyrosine phosphatase domain of PTPRR, and the rest express COOH-terminally truncated TEL due to frameshift. As judged from higher levels of amplification in RT-PCR analysis, two isoforms, tTEL (type 1) and TEL/PTPRR, are likely to be dominantly expressed in the leukemic cells. Generation of truncated form of TEL from the *TEL*-related chimeric allele is also reported in the *TEL/JAK2* chimeric gene (22). Importantly, whereas wild-type *TEL* mRNA is detected in the leukemic cells, neither reciprocal *PTPRR/TEL* nor wild-type *PTPRR* mRNA is detected in the sample. This suggests that promoter of the *PTPRR* gene is inactivated in these leukemic cells. These data indicate that tTEL and TEL/PTPRR are implicated in the pathogenesis of inv(12)-type leukemia.

To get some insight into the underpinning mechanisms in leukemogenesis by inv(12)(p13q13), we evaluated molecular functions of tTEL and TEL/PTPRR. Because TEL is a tumor suppressor, functional effects of the mutant proteins on wild-type TEL may be one cause of leukemia. We reported that ΔETS isoforms, which lack the ETS DNA-binding domain and are frequently expressed in acute myelogenous leukemia transformed from myelodysplastic syndrome, molecularly and biologically show dominant-negative effects over functions of wild-type TEL (41). As expected from their structural similarity in TEL part to ΔETS isoforms, both tTEL and TEL/PTPRR dominantly interfere with transcriptional repression mediated by wild-type TEL of both

−47−

artificial EBS reporter and endogenous *Bcl-X$_L$* gene. Thus, losing the ETS DNA-binding domain but retaining the helix-loop-helix domain seems critical to bolster the dominant inhibitory ability. Considering that both tTEL and TEL/PTPRR are found to heterodimerize with wild-type TEL, there are three plausible explanations for molecular basis of this effect. First, tTEL and TEL/PTPRR seem to prevent *de novo* translated wild-type TEL from entering the nucleus because wild-type TEL molecule resides mainly in the nucleus on its own, but almost equally in both the nucleus and the cytoplasm when coexpressed with the TEL mutants. Importantly, we observed the cytoplasmic localization of endogenous wild-type TEL in primary leukemic cells carrying inv(12). Second, TEL/PTPRR impairs DNA-binding property of wild-type TEL although tTEL does not. Third, tTEL and TEL/PTPRR may take corepressor mSin3A away from wild-type TEL because they associate with endogenous mSin3A in COS-7 cells (data not shown). The same dominant interfering functions of chimeric protein over authentic TEL have also been reported in TEL/AML1 by t(12;21)(p13;q22) in pediatric acute lymphoblastic leukemia (35) and provide one molecular mechanism (loss of tumor suppressive function of wild-type TEL) in leukemogenesis by 12p13 translocations. Given that Bcl-X$_L$ is an antiapoptotic molecule, its derepressed expression by the aberrant TEL proteins could be one of the molecular pathogeneses in inv(12)-type leukemia.

PTPRR is the first protein tyrosine phosphatase that was identified as a fusion partner for TEL. It is a receptor-type phosphatase possessing an intracellular catalytic domain at the COOH terminus (46–48). Due to alternative splicing or promoter switch, PTPRR exists as various isoforms in different organs such as brain, placenta, uterus, and colon (49, 50). However, there is no report that PTPRR is expressed in hematopoietic tissues. Notably, wild-type PTPRR is not expressed in the leukemic cells, and TEL/PTPRR does not show any phosphatase activity probably due to incomplete structure of the catalytic domain with loss of its NH$_2$-terminal part. These observations indicate that alteration in phosphatase activity is not causally related to leukemogenic mechanism in these cells. Despite this indication, one interesting hypothesis is that aberrant expression of a portion of catalytically inactive PTPRR in the chimeric form may protect some phosphorylated tyrosine residues that transmit growth-stimulating signals from dephosphorylation. As a result, this may constitutively activate proliferation-inducing pathways.

Employing factor-dependent UT7/GM cells, we explored the oncogenic potential of tTEL and TEL/PTPRR. Overexpression of TEL/PTPRR renders these cells factor independent, whereas overexpression of tTEL does not prevent apoptotic induction after factor deprivation. Therefore, TEL/PTPRR could exhibit transforming activity in myeloid cells, but tTEL alone could not, although tTEL may support the TEL/PTPRR activity. This suggests

that the dominant-negative effects over wild-type TEL are not sufficient in the development of leukemia. Interestingly, phosphorylated STAT3 does not fade away after factor withdrawal in both tTEL- and TEL/PTPRR-expressing cells, which is in sharp contrast to mock cells. All the other signaling molecules examined, such as ERK1/2 and JNK in MAP kinase pathway, Akt1/2/3 in phosphatidylinositol 3-kinase pathway, and STAT1 and STAT5 in JAK/STAT pathway, show no difference in phosphorylation levels among mock, tTEL-, and TEL/PTPRR-expressing cells both before and after factor removal. Because STAT3 is one of the well-known signal transducers involved in UT7/GM cell growth (51), the maintenance of phosphorylated STAT3 seems to contribute to the leukemic cell growth without GM-CSF. How these mutants preserve phosphorylated STAT3 remains unknown, but it could be possible for TEL/PTPRR to bind STAT3 through the helix-loop-helix domain of TEL and protect its phosphorylated tyrosine residues through the catalytically inactive domain of PTPRR, because it has been reported that wild-type TEL associates with STAT3 through the helix-loop-helix domain (52). Furthermore, wild-type TEL is found to repress STAT3-mediated transcriptional activity in the literature. Although we could not show the association between endogenous STAT3 and overexpressed tTEL or TEL/PTPRR in UT7/GM cells (data not shown), tTEL and TEL/PTPRR may stimulate the STAT3 signals by heterodimerizing with wild-type TEL and thus blocking its inhibitory functions on STAT3.

In summary, tTEL and TEL/PTPRR produced from the rearranged *TEL* allele could be important players in the development of leukemia carrying inv(12)(p13q13). They could block two functions of tumor-suppressive wild-type TEL: transcriptional repression through EBS and inhibition of STAT3-mediated signal. However, common functions of these two molecules may not be sufficient, if any, in the leukemogenesis because overexpression of tTEL does not induce autonomous cell growth of the factor-dependent cells by itself. The PTPRR part in TEL/PTPRR fusion protein might provide additional unknown functions for growth advantage. Further experiments with mouse modeling are needed to prove their leukemogenic roles *in vivo*.

Acknowledgments

References

1. Golub TR, Barker GF, Lovett M, Gilliland DG. Fusion of PDGF receptor β to a novel *ets*-like gene, *tel*, in chronic myelomonocytic leukemia with t(5;12) chromosomal translocation. Cell 1994; 77:307–16.

2. Poirel H, Oury C, Carron C, et al. The TEL gene products: nuclear phosphoproteins with DNA binding properties. Oncogene 1997;14:349–57.

3. Gu X, Shin BH, Akbarali Y, et al. Tel-2 is a novel transcriptional repressor related to the Ets factor Tel/ETV-6. J Biol Chem 2001;276:9421–36.

4. Kim CA, Phillips ML, Kim W, et al. Polymerization of the SAM domain of TEL in leukemogenesis and transcriptional repression. EMBO J 2001;20: 4173–82.

5. Kwiatkowski BA, Bastian LS, Bauer TR Jr, Tsai S, Zielinska-Kwiatkowska AG, Hickstein DD. The *ets* family member Tel binds to the Fli-1 oncoprotein and inhibits its transcriptional activity. J Biol Chem 1998;273:17525–30.

6. Potter MD, Buijs A, Kreider B, van Rompaey L, Grosveld G. Identification and characterization of a new human ETS-family transcription factor, *TEL2*, that is expressed in hematopoietic tissues and can associate with *TEL1/ETV6*. Blood 2000;95:3341–8.

7. Wang L, Hiebert SW. TEL contacts multiple corepressors and specifically associates with histone deacetylase-3. Oncogene 2001;20:3716–25.

—48—

8. Lopez RG, Carron C, Oury C, Gardellin P, Bernard O, Ghysdael J. TEL is a sequence-specific transcriptional repressor. J Biol Chem 1999;274:30132–8.

9. Martinez R, Golub TR. Transcriptional repression of Id1 by the leukemogenic ETS protein TEL [abstract]. Blood 2000;96:453a.

10. Fenrick R, Wang L, Nip J, et al. TEL, a putative tumor suppressor, modulates cell growth and cell morphology of Ras-transformed cells while repressing the transcription of *stromelysin-1*. Mol Cell Biol 2000;20:5828–39.

11. Irvin BJ, Wood LD, Wang L, et al. TEL, a putative tumor suppressor, induces apoptosis and represses transcription of Bcl-X$_L$. J Biol Chem 2003;278:46378–86.

12. Wang LC, Kuo F, Fujiwara Y, Gilliland DG, Golub TR, Orkin SH. Yolk sac angiogenesis defect and intra-embryonic apoptosis in mice lacking the Ets-related factor TEL. EMBO J 1997;16:4374–83.

13. Wang LC, Swat W, Fujiwara Y, et al. The TEL/ETV6 gene is required specifically for hematopoiesis in the bone marrow. Genes Dev 1998;12:2392–402.

14. Hock H, Meade E, Medeiros S, et al. Tel/Etv6 is an essential and selective regulator of adult hematopoietic stem cell survival. Genes Dev 2004;18:2336–41.

15. van Rompaey L, Potter M, Adams C, Grosveld G. Tel induces a G1 arrest and suppresses Ras-induced transformation. Oncogene 2000;19:5244–50.

16. Carroll M, Tomasson MH, Barker GF, Golub TR, Gilliland DG. The TEL/platelet-derived growth factor β receptor (PDGFβR) fusion in chronic myelomono-cytic leukemia is a transforming protein that self-associates and activates PDGFβR kinase-dependent signaling pathways. Proc Natl Acad Sci U S A 1996;93:14845–50.

17. Jousset C, Carron C, Boureux A, et al. A domain of TEL conserved in a subset of ETS proteins defines a specific oligomerization interface essential to the mitogenic properties of the PDGFβR oncoprotein. EMBO J 1997;16:69–82.

18. Eguchi M, Eguchi-Ishimae M, Tojo A, et al. Fusion of ETV6 to neurotrophin-3 receptor TRKC in acute myeloid leukemia with t(12;15)(p13;q25). Blood 1999;93:1355–63.

19. Papadopoulos P, Ridge SA, Boucher CA, Stocking C, Wiedemann LM. The novel activation of *ABL* by fusion to an *ets*-related gene, *TEL*. Cancer Res 1995;55:34–8.

20. Golub TR, Goga A, Barker GF, et al. Oligomerization of the ABL tyrosine kinase by the Ets protein TEL in human leukemia. Mol Cell Biol 1996;16:4107–16.

21. Lacronique V, Boureux A, Valle VD, et al. A TEL-JAK2 fusion protein with constitutive kinase activity in human leukemia. Science 1997;278:1309–12.

22. Peeters P, Raynaud SD, Cools J, et al. Fusion of *TEL*, the ETS-variant gene 6 (*ETV6*), to the receptor-associated kinase *JAK2* as a result of t(9;12) in a lymphoid and t(9;15;12) in a myeloid leukemia. Blood 1997;90:2535–40.

23. Kuno Y, Abe A, Emi N, et al. Constitutive kinase activation of the *TEL-Syk* fusion gene in myelodysplastic syndrome with t(9;12)(q22;p12). Blood 2001;97:1050–5.

24. Cazzaniga G, Tosi S, Aloisi A, et al. The tyrosine kinase *abl*-related gene *ARG* is fused to *ETV6* in an AML-M4Eo patient with a t(1;12)(q25;p13): molecular cloning of both reciprocal transcripts. Blood 1999;94:4370–3.

25. Golub TR, Barker GF, Bohlander SK, et al. Fusion of the *TEL* gene on 12p13 to the *AML1* gene on 21q22 in acute lymphoblastic leukemia. Proc Natl Acad Sci U S A 1995;92:4917–21.

26. Romana SP, Mauchauffé M, Le Coniat M, et al. The t(12;21) of acute lymphoblastic leukemia results in a tel-AML1 gene fusion. Blood 1995;85:3662–70.

27. Hiebert SW, Sun W, Davis JN, et al. The t(12;21) converts AML-1B from an activator to a repressor of transcription. Mol Cell Biol 1996;16:1349–55.

28. Fears S, Gavin M, Zhang DE, et al. Functional characterization of ETV6 and ETV6/CBFA2 in the regulation of the MCSFR proximal promoter. Proc Natl Acad Sci U S A 1997;94:1949–54.

29. Fenrick R, Amann JM, Lutterbach B, et al. Both TEL and AML-1 contribute repression domains to the t(12;21) fusion protein. Mol Cell Biol 1999;19:6566–74.

30. Buijs A, Sherr S, van Baal S, et al. Translocation (12;22)(p13;q11) in myeloproliferative disorders results in fusion of ETS-like *TEL* gene on 12p13 to the *MN1* gene on 22q11. Oncogene 1995;10:1511–9.

31. Buijs A, van Rompaey L, Molijn AC, et al. The MN1-TEL fusion protein, encoded by the translocation (12;22)(p13;q11) in myeloid leukemia, is a transcription factor with transforming activity. Mol Cell Biol 2000;20:9281–93.

32. Peeters P, Wlodarska I, Baens M, et al. Fusion of ETV6 to MDS1/EVI1 as a result of t(3;12)(q26;p13) in myeloproliferative disorders. Cancer Res 1997;57:564–9.

33. Cazzaniga G, Daniotti M, Tosi S, et al. The paired box domain gene *PAX5* is fused to *ETV6/TEL* in an acute lymphoblastic leukemia case. Cancer Res 2001;61:4666–70.

34. Chase A, Reiter A, Burci L, et al. Fusion of ETV6 to the caudal-related homeobox gene CDX2 in acute myeloid leukemia with the t(12;13)(p13;q12). Blood 1999;93:1025–31.

35. Gunji H, Waga K, Nakamura F, et al. TEL/AML1 shows dominant-negative effects over TEL as well as AML1. Biochem Biophys Res Commun 2004;322:623–30.

36. Baens M, Peeters P, Guo C, Aerssens J, Marynen P. Genomic organization of TEL: the human ETS-variant gene 6. Genome Res 1996;6:404–13.

37. Rowley JD, Diaz MO, Espinosa R III, et al. Mapping chromosome band 11q23 in human acute leukemia with biotinylated probes: Identification of 11q23 transloca-tion breakpoints with a yeast artificial chromosome. Proc Natl Acad Sci U S A 1990;87:9358–62.

38. Bohlander SK, Espinosa R III, Fernald AA, Rowley JD, Le Beau MM, Diaz MO. Sequence-independent ampli-fication and labeling of yeast artificial chromosomes for fluorescence *in situ* hybridization. Cytogenet Cell Genet 1994;65:108–10.

39. Arai H, Maki K, Waga K, et al. Functional regulation of TEL by p38-induced phosphorylation. Biochem Biophys Res Commun 2002;299:116–25.

40. Waga K, Nakamura Y, Maki K, et al. Leukemia-related transcription factor TEL accelerates differenti-ation of friend erythroleukemia cells. Oncogene 2003;22:59–68.

41. Sasaki K, Nakamura Y, Maki K, et al. Functional analysis of a dominant-negative ΔETS TEL/ETV6 isoform. Biochem Biophys Res Commun 2004;317:1128–37.

42. Maki K, Arai H, Waga K, et al. Leukemia-related transcription factor TEL is negatively regulated through extracellular signal-regulated kinase-induced phosphor-ylation. Mol Cell Biol 2004;24:3227–37.

43. Tanaka T, Tanaka K, Ogawa S, et al. An acute myeloid leukemia gene, *AML1*, regulates hemopoietic myeloid cell differentiation and transcriptional activation antag-onistically by two alternative spliced forms. EMBO J 1995;14:341–50.

44. Wood LD, Irvin BJ, Nucifora G, Luce KS, Hiebert SW. Small ubiquitin-like modifier conjugation regulates nuclear export of TEL, a putative tumor suppressor. Proc Natl Acad Sci U S A 2003;100:3257–62.

45. Chakrabarti SR, Sood R, Nucifora G. Posttranslational modification of TEL and TEL/AML1 by SUMO-1 and cell-cycle-dependent assembly into nuclear bodies. Proc Natl Acad Sci U S A 2000;97:13281–5.

46. Hendriks W, Schepens J, Brugman C, Zeeuwen P, Wieringa B. A novel receptor-type protein tyrosine phosphatase with a single catalytic domain is specif-ically expressed in mouse brain. Biochem J 1995;305:499–504.

47. Ogata M, Sawada M, Fujino Y, Hamaoka T. cDNA cloning and characterization of a novel receptor-type protein tyrosine phosphatase expressed predominantly in the brain. J Biol Chem 1995;270:2337–43.

48. Shiozuka K, Watanabe Y, Ikeda T, Hashimoto S, Kawashima H. Cloning and expression of *PCPTP1* encoding protein tyrosine phosphatase. Gene 1995;162:279–84.

49. Augustine KA, Silbiger SM, Bucay N, et al. Protein tyrosine phosphatase (PC12, Br7, S1) family: expression characterization in the adult human and mouse. Anat Rec 2000;258:221–34.

50. van den Maagdenberg AM, Bachner D, Schepens JT, et al. The mouse *Ptprr* gene encodes two protein tyrosine phosphatases, PTP-SL and PTPBR7, that display distinct patterns of expression during neural development. Eur J Neurosci 1999;11:3832–44.

51. Miura Y, Kirito K, Komatsu N. Regulation of both erythroid and megakaryocytic differentiation of a human leukemia cell line, UT-7. Acta Haematol 1998;99:180–4.

52. Schick N, Oakeley EJ, Hynes NE, Badache A. TEL/ETV6 is a signal transducer and activator of transcrip-tion 3 (Stat3)-induced repressor of Stat3 activity. J Biol Chem 2004;279:38787–96.

−49−

Dysplastic definitive hematopoiesis in *AML1/EVI1* knock-in embryos

Kazuhiro Maki, Tetsuya Yamagata, Takashi Asai, Ieharu Yamazaki, Hideaki Oda, Hisamaru Hirai, and Kinuko Mitani

The *AML1/EVI1* chimeric gene is created by the t(3;21)(q26;q22) chromosomal translocation seen in patients with leukemic transformation of myelodysplastic syndrome or blastic crisis of chronic myelogenous leukemia. We knocked-in the *AML1/EVI1* chimeric gene into mouse *Aml1* genomic locus to explore its effect in developmental hematopoiesis in vivo. *AML1/EVI1/+* embryo showed defective hematopoiesis in the fetal liver and died around embryonic day 13.5 (E13.5) as a result of hemorrhage in the central nervous system. The peripheral blood had yolk-sac–derived nucleated erythroblasts but lacked erythrocytes of the definitive origin. Although E12.5 fetal liver contained progenitors for macrophage only, E13.5 fetal liver contained multilineage progenitors capable of differentiating into dysplastic myelocyte and megakaryocyte. No erythroid progenitor was detected in E12.5 or E13.5 fetal liver. Hematopoietic progenitors from E13.5 *AML1/EVI1/+* fetal liver were highly capable of self-renewal compared with those from wild-type liver. Maintained expression of *PU.1* gene and decreased expression of *LMO2* and *SCL* genes may explain the aberrant hematopoiesis in *AML1/EVI1/+* fetal liver. (Blood. 2005;106:2147-2155)

© 2005 by The American Society of Hematology

Introduction

The t(3;21)(q26;q22) chromosomal translocation occurs in patients with aggressive transformation of myelodysplastic syndrome (MDS) or chronic myelogenous leukemia (CML).[1-4] In the joining region of t(3;21)(q26;q22), the *AML1* gene on 21q22 is fused with the *EVI1* (ecotropic viral integration site-1) gene on 3q26.[5] The resultant *AML1/EVI1* fusion gene is translated in frame to generate a chimeric transcription factor in which the N-terminal of AML1, including its DNA-binding Runt domain, is fused to almost the entire portion of EVI1. This chimeric transcription factor could be a molecular culprit for the leukemic progression of stem-cell malignancies caused by t(3;21)(q26;q22).

AML1 is involved in transcriptional regulation of a number of hematopoietic cell–specific genes. The Runt domain of AML1 binds to a specific DNA consensus sequence named polyomavirus enhancer binding protein 2 (PEBP2; ACCRCA), together with a non–DNA-binding β subunit (core-binding factor β [CBFβ]/ PEBP2β) to form a heterodimeric active transcription factor complex.[6-10] *AML1-* or *CBFβ*-deficient mice are embryonic lethal at embryonic day 12.5 (E12.5) and show massive hemorrhage in the central nervous system (CNS) with lack of hematopoiesis in the fetal liver.[11-15] A recent study demonstrated that inactivation of AML1 in adult mice results in megakaryocyte maturation arrest, defect in T- and B-lymphocyte development, and increase in hematopoietic precursor cells.[16]

The *EVI1* gene was initially identified as the frequent retrovirus integration site in myeloid tumors in AKXD mice.[17] EVI1 is less detected in normal hematopoietic cells but highly expressed in some patients of MDS or acute myelogenous leukemia (AML).[18,19]

EVI1 has 2 zinc finger domains, one in the N-terminal and the other in the C-terminal region. EVI1 is reported to interfere with the transforming growth factor β (TGFβ) signaling and to antagonize its growth inhibitory effect through targeting an intracellular signal transducer Smad3.[20] EVI1 is also known to enhance activator protein 1 (AP-1) activity[21] or block c-Jun N-terminal kinase (JNK) activity.[22] These findings suggest the versatile nature of this molecule in malignant transformation of hematopoietic cells.

The molecular characterization of AML1/EVI1 points to 2 major mechanisms of its leukemogenic effect; one is the dominant suppression of the functions of wild-type AML1, and the other is the ectopic expression of EVI1 molecule in the hematopoietic cells.[23] AML1/EVI1 binds to the PEBP2 site through its Runt domain and suppresses the expression of AML1 target genes by recruiting corepressor C-terminal binding protein by the EVI1 portion.[24,25] This dominant-negative effect is a common feature among AML1-related chimeric molecules, including AML1/ETO (eight-twenty-one) in t(8;21)(q22;q22) and translocation ets leukemia (TEL)/AML1 in t(12;21)(p13;q22).[9,23,26-29] By suppressing the expression of canonical AML1 target genes, AML1/EVI1 distorts the normal function of AML1 and may lead to leukemia development. The second mechanism of leukemogenesis is brought by the EVI1 part; inhibition of TGFβ signaling,[30] stimulation of AP-1 activity,[31] or repression of JNK activity.[22] Thus, EVI1 portion also contributes to the oncogenicity of AML1/EVI1.

Of the AML1-fusion proteins, AML1/EVI1 and AML1/ETO are of particular interest. They show a similar structure; N-terminal half of AML1, including the Runt domain, is fused to almost the

---

−50−

entire of EVI1 or ETO, both of which are the zinc finger protein.[23,28,29] Moreover, AML1/EVI1 and AML1/ETO mediate dominant-negative effects over wild-type AML1 by recruiting corepressors via EVI1[23] and ETO portions,[28,29] respectively. However, despite such similarities in molecular structure and function, AML1/EVI1 and AML1/ETO are differentially associated with the disease phenotype. AML1/EVI1 aggravates MDS or CML,[1-4] while AML1/ETO develops de novo AML subtype M2 of the French-American-British classification.[29] A possible explanation for such different disease settings is that AML1/EVI1 and AML1/ETO perturb different signaling pathway. Thus, exploring the molecular functional differences between AML1/EVI1 and AML1/ETO in vivo would advance our understanding toward differential role of the chimeric transcription molecules in causing different forms of leukemia.

For a direct comparison of AML1/EVI1– and AML1/ETO-expressing animals, we created *AML1/EVI1* knock-in mice and compared its phenotype with that of *AML1/ETO* knock-in mice described previously.[32,33] *AML1/EVI1/*[+] embryos died around E13.5 resulting from hemorrhage in the brain and the spinal cord as a result of impaired definitive hematopoiesis in the fetal liver. However, E13.5 fetal liver contained hematopoietic progenitors with enhanced replating efficiency. These phenotypes are shared between *AML1/EVI1/*[+] and *AML1/ETO/*[+] embryos. On the other hand, unique to *AML1/EVI1/*[+] mice was that hematopoietic progenitors in the fetal liver cannot develop to erythroid cells but can develop into dysplastic myeloid and megakaryocytic cells, whereas hematopoietic progenitors in the *AML1/ETO/*[+] fetal liver produce cells of all 3 lineages with normal morphology. Expression analysis for the crucial genes revealed that *AML1/EVI1/*[+] fetal liver maintained normal level of the *PU.1* gene expression, but lacked expression of the *LMO2* and *SCL* genes. Normal expression of the *PU.1* gene may support maintenance of the progenitor cells capable of differentiating into the myeloid and megakaryocytic lineages, and the low levels of *LMO2* and *SCL* genes expression could lead to blockade of erythroid differentiation in *AML1/EVI1/*[+] fetal liver. Dysplastic hematopoiesis seen in *AML1/EVI1/*[+] embryo partly recapitulates that observed in patients with the t(3;21)(q26;q22) translocation, indicating the pathogenic role for this chimeric protein in t(3;21)(q26;q22)-related leukemia.

Materials and methods

Construction of AML1/EVI1 knock-in targeting vector

Murine *Aml1* genome derived from a genomic library was amplified by polymerase chain reaction (PCR) method to produce a DNA fragment that includes intron 4 and the first 94 base pair (bp) of exon 5 with silent mutations at codons 519 and 522 of exon 5 creating a *Sac*II cleavage site. In the same fashion, another DNA fragment including the last 16 bp of human *AML1* exon 5 and 5′ part of subsequent *EVI1* sequence was also amplified using human *AML1/EVI1* cDNA[5] as a template to create a *Sac*II site by introducing silent mutations at identical codons. These 2 PCR products were subcloned into the human *AML1/EVI1* expression plasmid, pME18S-AML1/EVI1,[5] to give an in-frame fusion of the first 94 bp of murine *Aml1* exon 5 to the following portion of human *AML1/EVI1* cDNA (Figure 1A). The Neo-resistant gene derived from *pBK-Neo*[32] was added downstream of the *AML1/EVI1* sequence. A 4.1-kb (kilobase) *Xba*I-*Avr*II fragment from intron 4 and a 4.3-kb *Eco*RI fragment from intron 5 of murine *Aml1* genome were used for homologous recombination. To create the final targeting vector, the DNA fragment containing the previously mentioned sequences was inserted into the *Not*I and *Cla*I sites of pBluescript-DTA (diphtheria toxin-A gene), in which the *Dta* gene from pMC1DTApolyA (Stratagene, La Jolla, CA) was subcloned into the *Sal*I site of pBluescript. The construct was verified by restriction endonuclease mapping and DNA sequencing.

Production of chimeric mice

The linearized targeting vector (50 μg) was electroporated into TT2 embryonic stem (ES) cells.[34] G418-resistant clones were analyzed for homologous recombination by Southern analysis hybridizing *Eco*RI-digested DNA with a probe 5′ to the 5′ homologous sequence in the targeting vector and a *Neo* gene probe (Figure 1B). Heterozygous *AML1/EVI1/*[+] clones with undifferentiated morphology were injected into morulas of the ICR mouse strain. Chimeric males were bred with C57BL/6 females, and whole-body specimens of resultant embryos were analyzed for the presence of the knock-in allele by Southern analysis.

Visual inspection and histologic analysis

Embryos were removed from the uterus, dissected free from the fetal membranes, and inspected under a dissecting microscope for evidence of gross abnormalities. Embryos were fixed in formaldehyde solution and embedded in paraffin. The sections were stained with hematoxylin and eosin solution. Peripheral blood was collected in 10 mM EDTA (ethylenediaminetetraacetic acid), and smears were stained with Wright-Giemsa solution.

Histologic images were obtained on either an Olympus AX80 microscope (Olympus, Tokyo, Japan) equipped with an Olympus DP70 digital camera, a Nikon Eclipse E600 microscope (Nikon, Tokyo, Japan) equipped with an Olympus DP12 digital camera, or an Olympus IMT-2 microscope equipped with an Olympus DP12 digital camera. Each microscope was equipped with a 10 ×/.22 ocular lens. Images were cropped in Adobe Photoshop CS (Adobe Systems, San Jose, CA) and composed in Canvas 9 (Polaroid, Waltham, MA).

Cell culture, transfection, and induction of megakaryocytic differentiation

K562 cells were maintained in RPMI-1640 supplemented with 10% fetal calf serum. To obtain bulk transfectant of mock or the *AML1/EVI1* cDNA, 1 × 10^{7} K562 cells were electroporated with 50 μg pCXN2 or pCXN2-AML1/EVI1 at 380 V and 975 μF using Gene Pulser (Bio-Rad, Hercules, CA) and selected with 0.4 mg/mL G418 (Sigma-Aldrich, St Louis, MO). Resistant cells were screened for expression of AML1/EVI1 chimeric
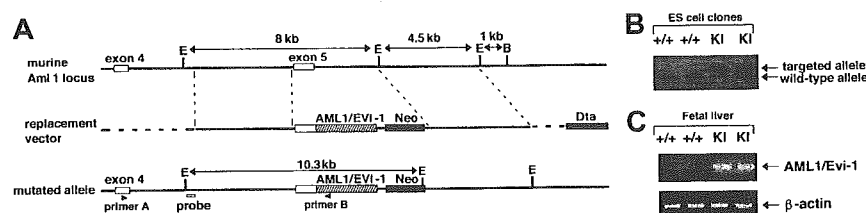
Figure 1. Gene targeting strategy to introduce AML1/EVI1 chimeric gene into the murine AML1 locus. (A) Schematic presentation of partial murine *Aml1* genomic locus (top line), replacement vector containing a partial human *AML1/EVI1* cDNA, a *neomycin resistance* cassette (Neo) for positive selection and a *diphtheria toxin-A* cassette (Dta) for negative selection (middle line), and the targeted allele (bottom line). (B) Southern analysis of wild-type (+/+) and *AML1/EVI1* knock-in (KI) ES cell clones. For detecting homologous recombination, the murine *Aml1*-specific probe indicated in the lower line of panel A was used. (C) RT-PCR analysis on E12.5 fetal liver cells from wild-type (+/+) and KI embryos. *AML1/EVI1* mRNA was amplified using primers A and B indicated in the lower line of panel A. Amplification was also performed for β-actin mRNA as a control for the presence of amplifiable RNA.

proteins by Western analysis using anti-AML1 Ab-1 antibody (Oncogene Research Products, San Diego, CA). To induce megakaryocytic differentiation, 100 nM staurosporine (Sigma-Aldrich) was added to the culture.

DNA content analysis

Each mock or AML1/EVI1–expressing K562 bulk population treated with 100 nM staurosporine was washed, fixed, and stained with 50 mg/mL propidium iodide using Cycle TEST PLUS (BD Biosciences, San Jose, CA). DNA content of nuclei was determined by fluorescence-activated cell sorting analysis.

Ultrastructural study

E13.5 fetal livers of *AML1/EVI1/*$^+$ heterozygous embryos and their wild-type littermates were examined with a JEOL 1200CX electron microscope (JEOL, Tokyo, Japan). Each mock or AML1/EVI1–expressing bulk population treated with 100 nM staurosporine for 48 hours was also examined.

In vitro culture of hematopoietic cells

Fetal livers from E12.5 or E13.5 embryos were disrupted by passing through 21-gage needles and then 26-gage needles for 3 times each. Single-cell suspensions with 1×10^4 cells were plated in triplicate in 1.2% methylcellulose in Iscoves modified Dulbecco medium containing 30% fetal calf serum, 0.1 mM β-mercaptoethanol, 2 mM glutamine, and 1% bovine serum albumin, 5 U/mL human erythropoietin, 100 ng/mL murine stem cell factor, 5 ng/mL murine interleukin 3 (IL-3; Kirin Brewery, Tokyo, Japan). Cell aggregates containing more than 50 cells were counted as colonies. Cytocentrifuge preparations of hematopoietic colonies were stained with Wright-Giemsa for morphologic examination, benzidine for the presence of erythroblasts, and choline esterase for the presence of megakaryocytes. In replating experiments, all of the cells from the preceding culture were collected, washed, and then replated at 1×10^4 cells per methylcellulose plate under the same condition as in the preceding culture. Colonies were scored as previously mentioned.

Quantitative reverse transcriptase (RT)–PCR analysis.

E12.5 and E13.5 live embryos were selected on the basis of the presence of heartbeats. Total RNA was isolated from liver cells using RNAeasy mini kit (Qiagen, Valencia, CA) according to the manufacturer's instructions. Random hexamer-primed cDNA was prepared from 2 μg total RNA with mouse mammary leukemia virus reverse transcriptase (Gibco BRL, Grand Island, NY) in a total volume of 25 μL. An oligonucleotide primer set containing murine *Aml1* exon 5–derived sense (5'-AAGAGCTTCACTCT-GACCAT-3') and human *EVI1* noncoding region–derived antisense (5'-CCTTTCACCTACTTCGATCT-3') sequences was used for amplification of the *AML1/EVI1* fusion sequence. Amplifications of various hematopoietic regulator transcripts were performed with primer sets described previously[35-39] as well as that for murine *CD11b*, sense (5'-CAGATCAA-CAATGTGACCGTATGG-3') and antisense (5'-CATCATGTCCTTGTACT-GCCGC-3') primers, using CYBR Green PCR Master Mix and ABI Prism 7700 Sequence Detector (Applied Biosystems, Foster, CA). Parallel reactions were carried out using a β-actin–amplifying primer set to ensure the integrity of the RNA samples.

Quantification of mRNA level was performed by measuring the cycle threshold (CT) that is defined as the fractional cycle number at which the fluorescence encounters a fixed threshold. The CT value of each gene was normalized to that of β-actin (ΔCT; CT value of target gene minus CT value of β-actin). Results were expressed as difference of ΔCT between *AML1/EVI1/*$^+$ versus wild-type or *AML1*$^{-/-}$ versus wild-type animals, and fold expression.

Results

Generation of an *AML1/EVI1* fusion allele

The t(3;21) breakpoint on chromosome 21 in human leukemic cells occurs in the fifth intron of the *AML1* gene, which is 3' to the exons

encoding the Runt DNA-binding domain.[5] To mimic in the mouse genome the mutant *AML1/EVI1* chimeric gene at the human t(3;21) allele, we made a targeting construct that replaces murine *Aml1* exon 5 with human *AML1* exon 5 fused in frame to the human *EVI1* sequence (Figure 1A). This targeting strategy renders generation of the murine/human hybrid *AML1/EVI1* gene whose expression is controlled by the endogenous mouse *Aml1* promoter. Using electroporation, we obtained 8 ES cell clones targeted correctly (no. 31, no. 35, no. 37, no. 42, no. 47, no. 50, no, 70, and no. 97), as determined by the presence of both *AML1/EVI1* allele and endogenous murine *Aml1* allele in Southern analysis (Figure 1B). These *AML1/EVI1/*$^+$ ES cell clones were injected into mouse morulas, and 2 chimeric mice (no. 31 and no. 97) transmitted the mutant allele through the germ line. These chimeric mice were largely healthy up to 7 months but showed sudden death thereafter. The cause of death is unknown despite anatomic examination performed immediately after the death of the 5 chimeric mice; there were no signs of hepatosplenomegaly or lymphadenopathy, excluding at least the leukemic cause of death.

Knock-in expression of *AML1/EVI1* fusion gene results in embryonic lethality with CNS hemorrhage and a lack of fetal-liver hematopoiesis

Genotyping analysis of 42 delivered F1 pups of *AML1/EVI1* chimeric male and wild-type C57BL/6 female found no *AML1/EVI1/*$^+$ genotypes, suggesting that *AML1/EVI1/*$^+$ embryos died in the uteri. *AML1*$^{+/+}$ agouti mice appeared normal; thus, designated major mutations did not occur in the ES cells. To examine the timing and cause of embryonic death in *AML1/EVI1/*$^+$ heterozygous embryos, we killed pregnant females at various time points between E10.5 and E14.5. The *AML1/EVI1* chimeric mRNA was detected in the fetal liver of the heterozygous mice by RT-PCR (Figure 1C). Between E10.5 and E11.5, all the *AML1/EVI1/*$^+$ embryos were viable and showed no significant morphologic abnormalities (Table 1). However, 10% of the embryos was found dead at E12.5 and 100% by E14.5, as judged by the absence of heart beats. The size of the *AML1/EVI1/*$^+$ embryos between E12.5 and E13.5 was comparable to that of the control littermates (Figure 2A). However, they had noticeable white livers, and signs of massive hemorrhage in the CNS and intersegmental regions of the presumptive spinal cord. Microscopic analysis revealed that the hemorrhage occurred as early as E12.5 in the cerebral ventricle and the dorsal root ganglia (Figure 2B-E), and such hemorrhagic sites were somewhat conserved in *AML1/EVI1/*$^+$ embryos analyzed (n = 58). This hemorrhage and lethality of *AML1/EVI1/*$^+$ heterozygous embryos were observed in 2 independent ES cell lines (no. 31 and no. 97). These data indicate that *AML1/EVI1/*$^+$ embryos die around E13.5 from the massive hemorrhage in the CNS. We focused our further analysis on embryos derived from line no. 97

**Table 1. Genotype and phenotype of embryos derived from AML1/EVI1 chimeric males mated with normal females**

Stages	No. of Pups	Genotype		Phenotype of KI* mice	
		+/+	+/KI*	Hemorrhage	Death
E10.5	9	1	8	0	0
E11.5	14	11	3	0	0
E12.5	98	67	31	27	3
E13.5	78	62	16	16	10
E14.5	32	21	11	11	11

Genotype analysis was performed by Southern analysis of DNA extracted from embryos. Surviving embryos were defined as those with beating hearts at the time of dissection.

*KI indicates AML1/EVI1 knock-in.
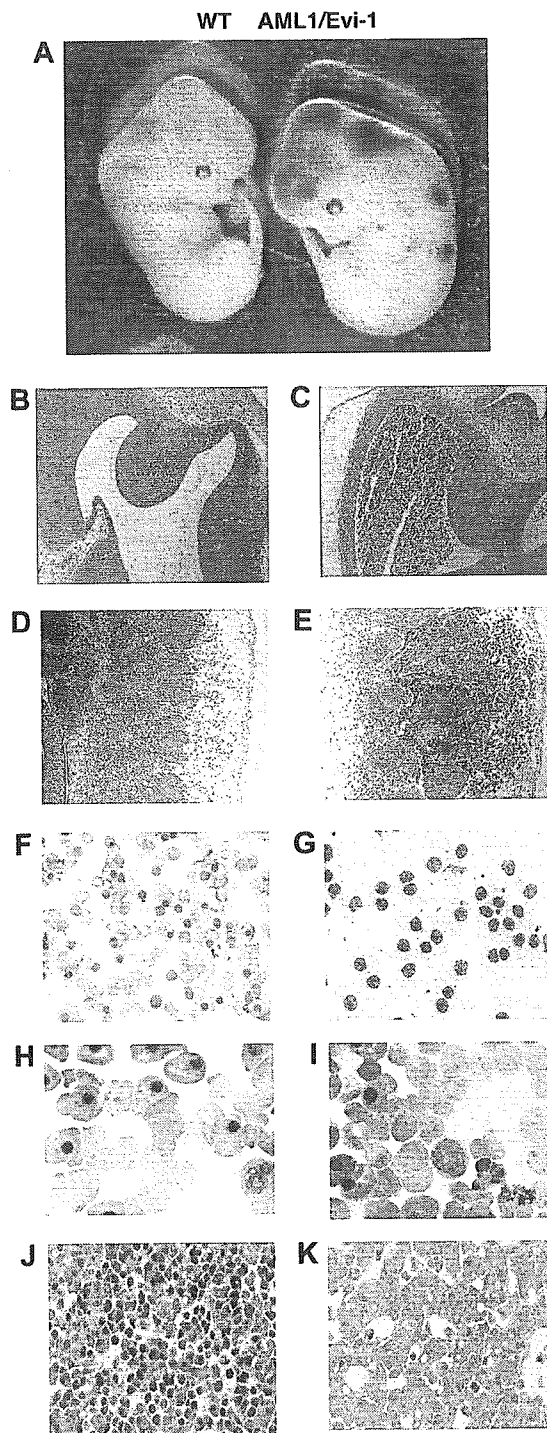
Figure 2. Morphologic comparison of E12.5 wild-type (WT) and AML1/EVI1/+ heterozygous embryos. (A) External appearance of WT and AML1/EVI1/+ littermates. AML1/EVI1/+ embryo on the right is similar in size to WT littermate on the left but is clearly identifiable by the presence of fetal liver pallor and massive hemorrhage within the CNS and soft tissues in the back (objective lens [OL], 2 ×/0.05; original magnification [OL], × 20). (B-C) Sections of the cerebral ventricle from WT (B) and AML1/EVI1/+ (C) embryos. AML1/EVI1/+ embryo shows massive hemorrhage into the ventricle (OL, 10 ×/0.40; OM, × 100). (D-E) Sections of the dorsal root ganglia from WT (D) and AML1/EVI1/+ (E) embryos. AML1/EVI1/+ embryo shows hemorrhage in the ganglia (OL, 10 ×/0.40; OM, × 100). (F-G) Smears of the peripheral blood from WT (F) and AML1/EVI1/+ (G) embryos. AML1/EVI1/+ embryo shows the absence of definitive erythrocytes, while WT littermate shows numerous enucleated definitive erythrocytes (OL, 40 ×/0.65; OM, × 400). (H-I) Smears of the peripheral blood from WT embryo. Only WT littermate shows monocyte (H) and neutrophil (I) (OL, 100 ×/1.40; OM, × 1000). (J-K) Sections of the fetal liver from WT (J) and AML1/EVI1/+ (K) embryos. AML1/EVI1/+ embryo shows a near complete absence of hematopoietic precursors, while WT littermate shows numerous hematopoietic precursor cells (OL, 20 ×/0.70; OM, × 200).
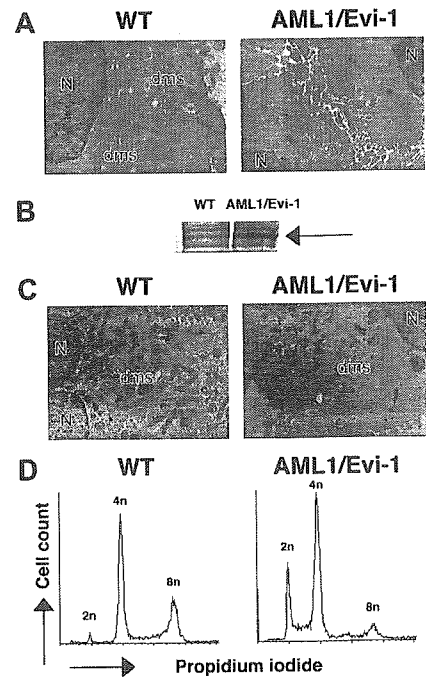
Figure 3. Morphology and DNA content of megakaryocytic cells overexpressing AML/EVI1. (A) Electron micrographs of megakaryocytes in E13.5 fetal liver. N indicates nucleus; dms, demarcation membrane (OM, × 3000). (B) Expression of AML1/EVI1 chimeric protein in transfected K562 cells. An arrow indicates overexpressed AML1/EVI1 proteins. (C) Electron micrographs of mock or AML1/EVI1–overexpressing K562 cells after staurosporine treatment for 48 hours. N indicates nucleus; dms, demarcation membrane (OM, × 3000). (D) DNA content of mock or AML1/EVI1–overexpressing K562 cells after staurosporine treatment for 48 hours.

because of the efficient germ line transmission and propagation relative to those from line no. 31.

Yolk sac hematopoiesis appeared largely intact in AML1/EVI1/+ embryos, with normal number and morphology of the yolk sac–derived nucleated erythroblasts circulating in the peripheral vessel (Figure 2G). Erythroblasts in E12.5 AML1/EVI1/+ embryos looked similar to those in E11.5 wild-type littermates, suggesting that they normally developed in the yolk sac. In contrast, fetal liver hematopoiesis was severely impaired, as indicated by markedly whitish liver resulting from a lack of red cells. The microscopic examination showed near complete absence of the erythroid, myeloid, or megakaryocytic progenitors of the definitive origin (Figure 2K). Postenucleated erythrocytes were absent in the peripheral blood from E12.5 AML1/EVI1/+ embryos, whereas it was abundantly observed in the peripheral blood of E12.5 wild-type littermates (Figure 2F-G). Also, monocytes and neutrophils were absent in the smears from AML1/EVI1/+ embryos, whereas they were easily observed in the smears from wild-type littermates (Figure 2H-I). These findings indicate that AML1/EVI1/+ heterozygous mice fail to establish definitive hematopoiesis in the fetal liver but maintain primary hematopoiesis in the yolk sac, recapitulating hematopoietic defects observed in AML1−/− [11,12] or AML1/ETO/+ mice.[32,33] We further performed electron microscopic examination to search for hematopoietic progenitors that would have been missed by histologic microscopic examination in the E13.5 fetal liver. In addition to decreased erythroid and myeloid progenitors, we observed megakaryocytes that were defective in their demarcation membrane (Figure 3A), which resemble those in AML1 conditional knock-out mice.[16] Thus, although there is massive defect in fetal liver hematopoiesis, some hematopoietic progenies do exist, although dysplastic, in the AML1/EVI1/+ fetal liver.

Table 2. Hematopoietic progenitors in E12.5 and E13.5 fetal liver

Stages/genotype	No. of Pups	BFU-E	CFU-GM	CFU-GEMM	CFU-M
E12.5					
+/+	13	10 ± 3	32 ± 8	20 ± 9	8 ± 2
AML1/EVI1/+	6	0	0	0	25 ± 11
E13.5					
+/+	9	8 ± 3	58 ± 14	25 ± 11	10 ± 3
AML1/EVI1/+	5	0	0	154 ± 54	4 ± 3

Numbers represent colonies per 1 × 10^4 fetal liver cells, mean ± SD.

BFU-E indicates erythroid burst-forming unit; CFU-GM, granulocyte/macrophage colony-forming unit; CFU-GEMM, granulocyte/erythrocyte/macrophage/megakaryocyte colony-forming unit; CFU-M, macrophage colony-forming unit.

To test for the direct effect of AML1/EVI1 molecule in megakaryocyte morphology, we expressed *AML1/EVI1* cDNA in human leukemic cell line K562 (Figure 3B) and differentiated one bulk population into the megakaryocytic lineage by exposing to staurosporine.[40] The AML1/EVI1–expressing K562 cells treated with staurosporine showed poorly developed demarcation membrane and lower level of polyploidy as compared with control mock cells (Figure 3C), indicating that the expression of AML1/EVI1 molecule is causative for the aberrant maturation of megakaryocytes in *AML1/EVI1*/+ mice.

AML1/EVI1 generates dysplastic hematopoietic progenitors in the fetal liver

To analyze for the defective hematopoiesis in the *AML1/EVI1*/+ embryos, we performed methylcellulose colony-forming assay using fetal liver cells from E12.5 or E13.5 embryos. Because the total number of cells recovered from E12.5 or E13.5 *AML1/EVI1*/+ fetal livers was 20-fold less than that recovered from wild-type fetal livers, we adjusted the number of plated fetal liver cells (1 × 10^4 cells) to assess for the precursor frequencies. In day 10 of culture, wild-type fetal liver gave rise to mutilineage colonies, whereas E12.5 *AML1/EVI1*/+ fetal liver cells generated macrophage colonies only, with no detectable erythroid, myeloid, and mixed colonies (Table 2). The E13.5 *AML1/EVI1*/+ cell culture looked similar to that of E12.5, except for some mixed-like colonies that were 5-fold more numerous than those from wild-type cell culture in microscopic examination. These data indicate that expression of AML1/EVI1 leads to severe defects in definitive hematopoiesis, but the fetal liver contains some progenitors capable of differentiating into multilineage hematopoietic progenies.

To gain more insights into the mixed–lineage-like colonies derived from E13.5 *AML1/EVI1*/+ fetal liver, we performed time-course microscopic analysis of the methylcellulose culture. On day 7 of culture, colonies from E13.5 *AML1/EVI1*/+ fetal liver

consisted mainly of myelocytic blastoid cells, while those from wild-type fetal liver contained numerous erythroblasts, hypergranular myeloid cells, and megakaryocytes (Figure 4). Benzidine staining confirmed the absence of erythroblasts in *AML1/EVI1*/+ cell-derived colonies. However, choline esterase–positive megakaryocytes were observed in both types of the colonies. On day 10, colonies from *AML1/EVI1*/+ fetal liver contained a large number of dysplastic myelocytes with bilobulated or multilobulated nuclei along with scanty cytoplasmic granulation. These findings suggest that hematopoietic progenitors in the *AML1/EVI1*/+ fetal liver are completely blocked for differentiation into the erythroid lineage but are capable of differentiating into the myeloid and megakaryocyte lineages, although immature and dysplastic.

Hematopoietic progenitor in the *AML1/EVI1*/+ fetal liver is highly capable of self-renewal

To examine self-renewal capacity of hematopoietic progenitors in the E13.5 *AML1/EVI1*/+ fetal liver, we performed a serial methylcellulose replating assay using bulk population of fetal liver–derived colonies under the conditions optimal for the development of multipotential hematopoietic progenitors. Cells from *AML1/EVI1*/+ fetal livers were able to replate beyond 7 passages, whereas cells from wild-type fetal livers lost their ability to form colonies after 5 passages (Table 3). During each replating, AML1/EVI1–expressing colonies showed increase in size and number (Figure 5, left). The cytospin samples from the fourth passage colony identified a polymorphic population of dysplastic cells, including agranular myelocytes and megakaryocytes (Figure 5, right). We conclude that expression of AML1/EVI1 in the fetal liver produces multilineage potential progenitors that are capable of more self-renewal than the wild-type progenitors and have a dysplastic maturation tendency. However, even after amplification of the cells through passage, we failed to demonstrate expression of AML1/EVI1 chimeric proteins in the colony-forming cells by Western analysis with anti-AML1 antibody, possibly because of low expression and high molecular weight (190 kDa) of the proteins.

Expression of *PU.1* is maintained in *AML1/EVI1*/+ fetal liver cells but significantly decreased in *AML1*−/− cells

To get the molecular underpinning for the dysregulated hematopoiesis caused by AML1/EVI1, we assessed the expression of various genes implicated in definitive hematopoiesis. The total RNA was extracted from E12.5 fetal liver cells from wild-type, *AML1*−/−, and *AML1/EVI1*/+ embryos, and mRNA was quantified using semiquantitative RT-PCR analysis. The level of expression in
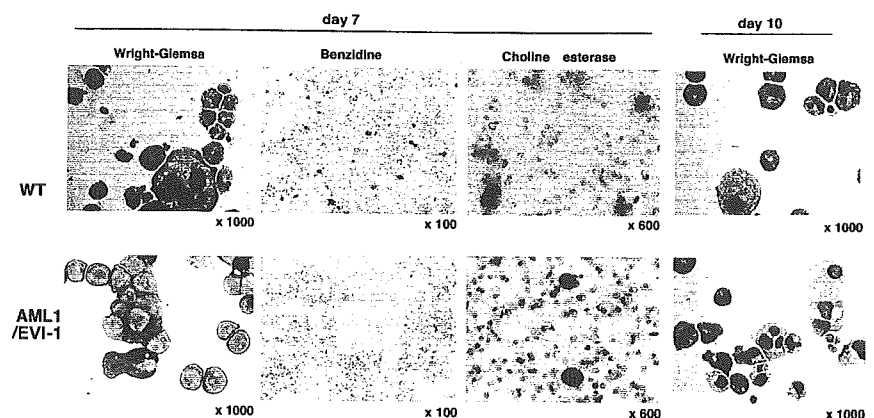
Figure 4. Morphology of dysplastic mixed-like hematopoietic colonies in the AML1/EVI1/+ fetal liver culture. On days 7 and 10 of culture, cytocentrifuge preparations of cells from mixed-like colonies were stained with Wright-Giemsa for morphologic examination (OL, 100 ×/1.40; OM, × 1000), benzidine for the presence of erythroblasts (OL, 10 ×/0.30; OM, × 100), or choline esterase for the presence of megakaryocytes (OL, 60 ×/1.40; OM, × 600). *AML1/EVI1*/+ mixed-like colonies in the bottom panels show retarded maturation and hypogranulation of myeloid cells as well as the absence of erythroid cells. In contrast, WT mixed colonies in the top panels show normal trilineage differentiation.

Table 3. Serial in vitro replating assays of E13.5 fetal liver hematopoietic progenitors

Genotype	In vitro passage						
	1	2	3	4	5	6	7
+/+	99 ± 23	384 ± 86	164 ± 41	59 ± 76	11 ± 9	0	0
AML1/EVI1/+	162 ± 59	388 ± 131	365 ± 150	403 ± 89	436 ± 104	407 ± 114	626 ± 3

Cells from methylcellulose culture were disaggregated, washed, and replated at 1 × 10⁴ cells per methylcellulose plate under the same condition every 7 days. Numbers represent colonies per 1 × 10⁴ cells, mean ± SD.

$AML1^{-/-}$ and $AML1/EVI1^{/+}$ fetal liver cells was compared with that in wild-type cells. Table 4 revealed the calculated fold expression of the indicated genes in $AML1^{-/-}$ and $AML1/EVI1^{/+}$ embryos relative to that of wild-type littermates along with the cycle threshold differences. The expression of the $PU.1$[41] gene in $AML1/EVI1^{/+}$ fetal liver cells was maintained to the normal, whereas its expression level was markedly decreased in $AML1^{-/-}$ fetal liver cells, as has been reported previously.[42] Consistent with this, the expression of the $CD11b$ gene, one of the target genes of PU.1 (an ets transcription factor family member), was maintained in $AML1/EVI1^{/+}$ knock-in liver, whereas markedly decreased in $AML1^{-/-}$ liver. The expression of the critical transcription factor such as PU.1 in $AML1/EVI1^{/+}$ fetal liver may support multilineage hematopoietic progenitors up to E13.5 and also aids the monocyte/macrophage lineage differentiation. The myeloid lineage-specific transcription factor $C/EBPA$[43] was expressed several fold higher in $AML1/EVI1^{/+}$ fetal liver cells than in wild-type cells, and this may bolster the myeloid-lineage differentiation along with PU.1. The expression levels of cytokine receptors transcripts such as G-CSF receptor and GM-CSF receptor were largely unchanged across wild-type, $AML1^{-/-}$ and $AML1/EVI1^{/+}$ fetal liver cells. On the other hand, the expression of erythroid lineage–specific genes such as $LMO2$[44] and SCL[45] was approximately 10-fold lower in $AML1/EVI1^{/+}$ fetal liver cells than in wild-type cells. The decreased expression of $LMO2$ and SCL could impinge on successful differentiation along the erythroid lineage in $AML1/EVI1^{/+}$ fetal liver cells, and the similar decrease was observed in $AML1^{-/-}$ fetal liver cells that lack erythroid cells as well. Other erythroid lineage–specific transcripts such as δ-aminolevulinic acid synthase-erythroid *(ALASE)* and β-globin were more decreased in $AML1/EVI1^{/+}$ fetal liver cells than in $AML1^{-/-}$ cells, despite equivalent expression of their master regulator GATA binding protein 1 (GATA-1) in both cell types. The net GATA-1 activity was presumably repressed in $AML1/EVI1^{/+}$ fetal liver cells because of

maintained expression of PU.1 that inhibits DNA binding of GATA-1.[46] The suppressed expression of *ALASE* and β-globin could also contribute to the complete defect of erythroid differentiation in $AML1/EVI1^{/+}$ progenitor cells. These expression analyses provide a logical explanation for the distinct hematopoietic capacity intrinsic to $AML1^{-/-}$ and $AML1/EVI1^{/+}$ fetal liver cells. Our data point that the sufficient expression of the $PU.1$ gene may be the first critical prerequisite for the definitive hematopoiesis to be set off in the fetal liver.
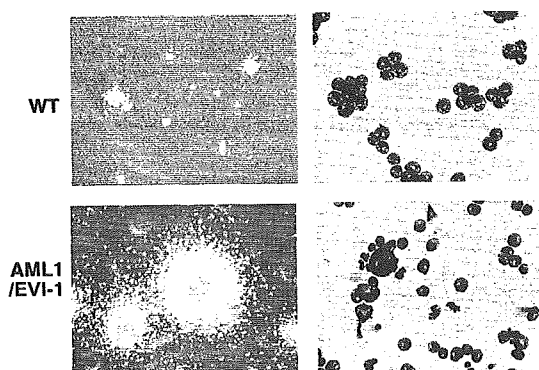
Discussion

AML1-CBFβ transcription factor complex is one of the critical regulators of the hematopoietic system. A substantial amount of evidence highlights the central role for this transcription factor system in normal hematopoiesis as well as in abnormal hematopoietic disorders. Four gene-ablated animals including ours, *AML1*-null,[11,12] *CBFB*-null,[13-15] *AML1/ETO* knock-in,[32,33] and *AML1/EVI1* knock-in mice, show normal hematopoiesis in the yolk sac but share common defects in definitive hematopoiesis in the fetal liver. These 4 embryos also show massive hemorrhage in the CNS and spinal cord and die during midgestation. A series of biochemical analyses in AML1-CBFβ transcription factor, or AML1/ETO or AML1/EVI1 fusion molecules[23,28,29] indicate that such in vivo phenotypes arise from shutting off or suppressing AML1 function in the early hematopoietic tissues. We speculate that such phenotype in *AML1/EVI1* knock-in mice also comes from dominant-negative effect against wild-type-AML1 in vivo.

The microscopic analysis of the fetal liver of the 4 mutant embryos shows common lack of visible hematopoietic cells.

Figure 5. Morphology of serially replated AML1/EVI1/⁺ hematopoietic colonies. (Left) WT and typical dysplastic multilineage $AML1/EVI1^{/+}$ colonies after the fourth passage. The size of $AML1/EVI1^{/+}$ hematopoietic colonies is significantly larger than that of WT colonies. (Right) Wright-Giemsa–stained cytocentrifuge preparations of the WT and $AML1/EVI1^{/+}$ colony. $AML1/EVI1^{/+}$ hematopoietic colonies maintain the dysplastic nature. Scales bars equal 300 μm (OL, 100 ×/1.40; OM, × 1000).

Table 4. Expressional changes of various hematopoietic regulators in E12.5 $AML1/EVI1^{/+}$ and $AML1^{-/-}$ fetal liver cells

	$\Delta CT_{KI} - \Delta CT_{WT}$	Fold (KI/WT)	$\Delta CT_{KO} - \Delta CT_{WT}$	Fold (KO/WT)
C/EBPA	-1.4 ± 0.1	2.7 ± 0.1	-2.9 ± 0.0	7.2 ± 0.1
LMO2	3.5 ± 0.3	0.1 ± 0.6	3.3 ± 0.1	0.1 ± 0.3
SCL	3.9 ± 0.8	0.1 ± 1.7	2.4 ± 0.2	0.2 ± 0.3
c-MYB	-0.5 ± 0.2	1.4 ± 1.5	-2.4 ± 0.3	5.4 ± 0.6
GATA1	-0.4 ± 0.7	1.4 ± 1.3	-1.6 ± 0.5	3.0 ± 1.0
PU.1	-0.4 ± 0.1	1.3 ± 0.1	8.2 ± 0.1	0.0 ± 0.3
NFE2	2.9 ± 0.5	0.1 ± 1.0	0.3 ± 0.2	0.6 ± 0.2
CD11b	1.2 ± 0.4	0.4 ± 0.8	5.0 ± 1.8	0.0 ± 3.6
MCSFR	0.1 ± 0.2	0.9 ± 0.4	-1.5 ± 0.9	2.8 ± 1.8
GCSFR	-0.6 ± 0.1	1.5 ± 0.2	0.0 ± 0.0	1.0 ± 0.0
GMCSFR	0.1 ± 0.2	1.1 ± 0.4	-0.6 ± 0.1	1.5 ± 0.2
MPO	10 ± 1.1	0.0 ± 2.2	7.0 ± 0.7	0.0 ± 1.3
β-globin	3.9 ± 0.9	0.1 ± 1.7	1.0 ± 0.4	0.5 ± 0.8
FOG1	2.3 ± 0.2	0.2 ± 0.3	2.0 ± 0.2	0.3 ± 0.3
ALASE	5.6 ± 0.4	0.0 ± 0.7	1.9 ± 0.4	0.3 ± 0.8

ΔCT indicates mean CT of indicated gene − mean CT of β-actin; KI, AML1/EVI1 knock-in; KO, AML1 knock-out; fold, fold difference relative to that of WT litters calculated by $2^{-(\Delta CT_{KI \text{ or } KO} - \Delta CT_{WT})}$. Data are means ± standard deviation.

Despite such gross similarity, close examination of the hemato-poiesis reveals some intriguing differences. First, although *AML1*[−/−][11,12] or *CBFB*[−/−][13-15] fetal liver has no hematopoietic progenitors that would have produced colonies, *AML1/EVI1/*[+] and *AML1/ETO/*[+32,33] fetal livers have progenitors that can give rise to macrophage colonies. *AML1/EVI1/*[+] fetal liver (E12.5) contains 3-fold more progenitors than wild-type fetal liver capable of differentiating into the monocyte/macrophage lineage, and a simi-lar finding is reported for *AML1/ETO/*[+] yolk sac where Yergeau et al[32] observed a marked increase in the number of macrophage colonies. Therefore, the capacity to differentiate along the monocyte/macrophage lineage seems a characteristic feature of hematopoietic progenitors expressing AML1/EVI1 or AML1/ETO in the fetal hematopoietic system. Second, in contrast to *AML1*^{−/−} or *CBFB*^{−/−} fetal liver, *AML1/EVI1/*[+] and *AML1/ETO/*[+33] fetal livers (E13.5) can also give rise to colonies committed to erythrocyte/megakaryo-cyte and myelocyte lineages. The appearance of megakaryocytic cells in the colony assay would suggest some production of platelets in these embryos, and this might contribute to 1 day-longer survival of *AML1/EVI1* and *AML1/ETO* knock-in embryos (lethal at E13.5) than *AML1* or *CBFB* knock-out embryos (lethal at E12.5). Third, the serial colony-forming assay demonstrates that AML1/EVI1− or AML1/ETO[33]-expressing progenitors show more self-renewal than those of the wild-type animals, although these progenitors cannot establish functional hematopoiesis in the fetal liver. These differences between AML1/EVI1− or AML1/ETO-expressing cells versus *AML1* or *CBFB* knock-out cells may arise from either incomplete suppression of wild-type-AML1 or addi-tional functions brought by the individual fused molecules.

Although *AML1/EVI1/*[+] and *AML1/ETO/*[+] fetal liver showed similar results in colony counts, there are some striking differences in their contents of colonies that are unlikely to result from minor differences in culture conditions. We used higher concentrations of erythropoietin and stem cell factor than those reported in *AML1/ETO/*[+] fetal liver culture.[32,33] Nonetheless, *AML1/EVI1/*[+] hemato-poietic progenitors fail to generate erythroid cells, whereas *AML1/ETO/*[+] hematopoietic progenitors give rise to mixed colonies containing numerous erythroblasts.[33] The observed resistance to the erythroid-lineage differentiation is highly characteristic of *AML1/EVI1/*[+] hematopoietic progenitors. This is consistent with the reported retroviral expression of EVI1 in hematopoietic progeni-tor cells that blocks erythroid differentiation in vitro[47] or the transgenic expression of EVI1 impairing erythropoiesis in vivo.[48] Therefore, the expression of EVI1, either in canonical form or as the fusion chimeric protein, is detrimental to erythroid-lineage differentiation. Another distinct finding between the 2 cell types is the more severe dysplasticity in *AML1/EVI1/*^{+} cells. In *AML1/EVI1/*[+] progenitors, the arising myeloid cells arrest at the myelo-cyte stage with no granulation, and the arising megakaryocytes show ill-developed demarcation membrane in the cytoplasm. In contrast, *AML1/ETO/*[+] progenitors exhibited far more differenti-ated morphologies, although reported dysplastic in the text.[33] Overexpressed EVI1 protein in G-CSF–treated 32Dcl3 cells com-pletely blocks myeloid differentiation.[49] Thus, the adverse effect of EVI1 in myeloid differentiation may contribute to the more severe defect in the myeloid maturation of the AML1/EVI1–expressing progenitors than that of the AML1/ETO-expressing cells. Finally, the abnormal expression of the *AML1/EVI1* gene causes distur-bance of megakaryocytic maturation, which is not observed in AML1/ETO-expressing animals. This effect seems direct as evi-dent by AML1/EVI1–expressing K562 cells showing poor demar-cation membrane and lower DNA ploidy when treated with staurosporine. In this case, however, the result seems to be caused by the dominant-negative effect over wild-type-AML1, as *AML1* conditional knock-out mice show similar maturation abnormality in megakaryocytes.

AML1/EVI1 causes broad perturbation of gene expression that is key to normal hematopoietic cell development. The first key gene is *PU.1* that is known to play a pivotal role in B cell/monocyte development[50-54] and the maintenance of hematopoietic stem cell in the fetal liver.[55] *PU.1* transcripts are markedly decreased in *AML1*^{−/−} fetal liver cells, as reported previously,[42] whereas its expression is normal in *AML1/EVI1/*[+] fetal liver cells, and this expression pattern is paralleled by one of its direct target gene *CD11b*. The maintained expression of PU.1 may afford *AML1/EVI1/*[+] hematopoietic progenitors a capacity to produce macro-phage and mixed colonies. Importantly, our data suggest that the reported complete lack of hematopoietic progenitors in *AML1*^{−/−} fetal liver may result from the absence of PU.1, and the recent finding underscores the critical role for PU.1 in supporting hematopoietic stem cell maintenance in the fetal liver.[55] Thus, PU.1 seems to be the key transcription factor that explains the pheno-typic difference between *AML1/EVI1/*[+] and *AML1*^{−/−} animals. The second key gene *CEBPA* is involved in early granulocytic differen-tiation.[56] The expression of *CEBPA* is increased in both *AML1/EVI1/*[+] and *AML1*^{−/−} fetal livers. In *AML1/EVI1/*[+] liver, the increased expression of C/EBPα may enhance myeloid/monocytic differentiation of the existing hematopoietic progenitor supported by PU.1. In *AML1*^{−/−} fetal liver, however, the lack of PU.1 expression dissipates the hematopoietic progenitor; thus, there is no myeloid/monocytic progeny arising from even the increased expres-sion of C/EBPα. Third, the expression of *LMO2* and *SCL* is severely repressed in *AML1/EVI1/*[+] fetal liver. The *LMO2* and *SCL* genes are essential for erythroid lineage differentiation,[44,45] and low expression of these genes could account for the absence of erythroid cells in *AML1/EVI1/*[+] fetal liver, even though the hematopoietic progenitor cells are supported by the presence of PU.1. The lack of *LMO2* and *SCL* expression is also observed in *AML1*^{−/−} fetal liver. This suggests that the defective expression of *LMO2* and *SCL* in *AML1/EVI1/*^{+} cells is due to dominant-negative effect of AML1/EVI1 over wild-type AML1, and that *LMO2* and *SCL* might be candidate target genes for wild-type AML1. This possibility might be worth exploring, although no PEBP2 binding sites are found at least in the proximal regulatory region of the *LMO2* or *SCL* gene.[57,58] Finally, it is worth emphasizing that *GATA1* expression is kept comparable across wild-type, *AML1*^{−/−}, and *AML1/EVI1/*[+] fetal livers, and yet its target genes *ALASE* and β-globin are much more repressed in *AML1/EVI1/*[+] fetal liver cells than in *AML1*^{−/−} cells. These differences in expression of *ALASE* and β-globin genes could be due to the interplay between PU.1 and GATA-1,[46] providing a case that some of the altered gene expres-sions are the consequences of the combinatory effect of involved transcription factors.

In summary, we have demonstrated that *AML1/EVI1* knock-in mice almost completely lack effective hematopoiesis in the fetal liver, but they retain progenitors with increased self-renewal capacity and potential to differentiate into the myeloid/monocytic and megakaryocytic lineages with some dysplasticity. We provide correlative evidence that PU.1 plays a critical role in the mainte-nance of hematopoietic progenitors in the *AML1/EVI1/*[+] fetal liver. Collectively, our study suggests that AML1/EVI1 is not only a

dominant-negative suppressor of wild-type-AML1 but also has more a proliferative and dysplastic effect added on by the fusing EVI1 part. Clinical evidence shows that the emergence of *AML1/EVI1* is associated with the progression of hematopoietic stem cell disorder, and our results explain the aggressive and dysplastic transformation of the disease course observed in patients with AML1/EVI1–expressing leukemia. Inducible expression of AML1/ETO in mouse hematopoietic tissue shows that the expression of AML1/ETO per se is not leukemogenic[59,60] and requires a second hit introduced by alkylating agents to cause leukemia.[60,61] It certainly needs to be tested whether the expression of AML1/EVI1 is sufficient to cause leukemia when expressed in an inducible fashion in adult mice. Our prediction would be that AML1/EVI1 expression is leukemogenic on its own, or at least more prone to leukemia when a second hit comes in. A conditional project of *AML1/EVI1* knock-in expression is in progress in our laboratory.

References

1. Rubin CM, Larson RA, Bitter MA, et al. Association of a chromosomal 3;21 translocation with the blast phase of chronic myelogenous leukemia. Blood. 1987;70:1338-1342.

2. Coyle T, Najfeld V. Translocation (3;21) in Philadelphia chromosome-positive chronic myelogenous leukemia prior to the onset of blast crisis. Am J Hematol. 1988;27:56-59.

3. Rubin CM, Larson RA, Anastasi J, et al. t(3;21)(q26;q22): a recurring chromosomal abnormality in therapy-related myelodysplastic syndrome and acute myeloid leukemia. Blood. 1990;76:2594-2598.

4. Schneider NR, Bowman WP, Frenkel EP. Translocation (3;21)(q26;q22) in secondary leukemia. Report of two cases and literature review. Ann Genet. 1991;34:256-263.

5. Mitani K, Ogawa S, Tanaka T, et al. Generation of the AML1-EVI-1 fusion gene in the t(3;21)(q26;q22) causes blastic crisis in chronic myelocytic leukemia. EMBO J. 1994;13:504-510.

6. Ito Y. Oncogenic potential of the RUNX gene family: "overview." Oncogene. 2004;23:4198-4208.

7. van Wijnen AJ, Stein GS, Gergen JP, et al. Nomenclature for Runt-related (RUNX) proteins. Oncogene. 2004;23:4209-4210.

8. Levanon D, Groner Y. Structure and regulated expression of mammalian RUNX genes. Oncogene. 2004;23:4211-4219.

9. Durst KL, Hiebert SW. Role of RUNX family members in transcriptional repression and gene silencing. Oncogene. 2004;23:4220-4224.

10. Cameron ER, Neil JC. The Runx genes: lineage-specific oncogenes and tumor suppressors. Oncogene. 2004;23:4308-4314.

11. Okuda T, van Deursen J, Hiebert SW, Grosveld G, Downing JR. AML1, the target of multiple chromosomal translocations in human leukemia, is essential for normal fetal liver hematopoiesis. Cell. 1996;84:321-330.

12. Wang Q, Stacy T, Binder M, Marin-Padilla M, Sharpe AH, Speck NA. Disruption of the Cbfa2 gene causes necrosis and hemorrhaging in the central nervous system and blocks definitive hematopoiesis. Proc Natl Acad Sci U S A. 1996;93:3444-3449.

13. Wang Q, Stacy T, Miller JD, et al. The CBFβ subunit is essential for CBFα2 (AML1) function in vivo. Cell. 1996;87:697-708.

14. Sasaki K, Yagi H, Bronson RT, et al. Absence of fetal liver hematopoiesis in mice deficient in transcriptional coactivator core binding factor β. Proc Natl Acad Sci U S A. 1996;93:12359-12363.

15. Niki M, Okada H, Takano H, et al. Hematopoiesis in the fetal liver is impaired by targeted mutagenesis of a gene encoding a non-DNA binding subunit of the transcription factor, polyomavirus enhancer binding protein 2/core binding factor. Proc Natl Acad Sci U S A. 1997;94:5697-5702.

16. Ichikawa M, Asai T, Saito T, et al. (Author list corrected in Erratum. Nat Med. 2005;11:102). AML-1 is required for megakaryocytic maturation and lymphocytic differentiation, but not for maintenance of hematopoietic stem cells in adult hematopoiesis. Nat Med. 2004;10:299-304.

17. Morishita K, Parker DS, Mucenski ML, Jenkins NA, Copeland NG, Ihle JN. Retroviral activation of a novel gene encoding a zinc finger protein in IL-3-dependent myeloid leukemia cell lines. Cell. 1988;54:831-840.

18. Morishita K, Parganas E, William CL, et al. Activation of EVI1 gene expression in human acute myelogenous leukemias by translocations spanning 300-400 kilobases on chromosome band 3q26. Proc Natl Acad Sci U S A. 1992;89:3937-3941.

19. Ogawa S, Kurokawa M, Tanaka T, et al. Increased Evi-1 expression is frequently observed in blastic crisis of chronic myelocytic leukemia. Leukemia. 1996;10:788-794.

20. Kurokawa M, Mitani K, Irie K, et al. The oncoprotein Evi-1 represses TGF-β signalling by inhibiting Smad3. Nature. 1998;394:92-96.

21. Tanaka T, Nishida J, Mitani K, Ogawa S, Yazaki Y, Hirai H. Evi-1 raises AP-1 activity and stimulates c-fos promoter transactivation with dependence on the second zinc finger domain. J Biol Chem. 1994;269:24020-24026.

22. Kurokawa M, Mitani K, Yamagata T, et al. The evi-1 oncoprotein inhibits c-Jun N-terminal kinase and prevents stress-induced cell death. EMBO J. 2000;19:2958-2968.

23. Mitani K. Molecular mechanisms of leukemogenesis by AML1/EVI-1. Oncogene. 2004;23:4263-4269.

24. Tanaka T, Mitani K, Kurokawa M, et al. Dual functions of the AML1/Evi-1 chimeric protein in the mechanism of leukemogenesis in t(3;21) leukemias. Mol Cell Biol. 1995;15:2383-2392.

25. Izutsu K, Kurokawa M, Imai Y, et al. The t(3;21) fusion product, AML1/Evi-1 blocks AML1-induced transactivation by recruiting CtBP. Oncogene. 2002;21:2695-2703.

26. Hiebert SW, Sun W, Davis JN, et al. The t(12;21) translocation converts AML-1B from an activator to a repressor of transcription. Mol Cell Biol. 1996;16:1349-1355.

27. Fenrick R, Amann JM, Lutterbach B, et al. Both TEL and AML-1 contribute repression domains to the t(12;21) fusion protein. Mol Cell Biol. 1999;19:6566-6574.

28. Nimer SD, Moore MA. Effects of the leukemia-associated AML1-ETO protein on hematopoietic stem and progenitor cells. Oncogene. 2004;23:4249-4254.

29. Peterson LF, Zhang DE. The 8;21 translocation in leukemogenesis. Oncogene. 2004;23:4255-4262.

30. Kurokawa M, Mitani K, Imai Y, Ogawa S, Yazaki Y, Hirai H. The t(3;21) fusion product, AML1/Evi-1, interacts with Smad3 and blocks transforming growth factor-β-mediated growth inhibition of myeloid cells. Blood. 1998;92:4003-4012.

31. Kurokawa M, Ogawa S, Tanaka T, et al. The AML1/Evi-1 fusion protein in the t(3;21) translocation exhibits transforming activity on Rat1 fibroblasts with dependence on the Evi-1 sequence. Oncogene. 1995;11:833-840.

32. Yergeau DA, Hetherington CJ, Wang Q, et al. Embryonic lethality and impairment of haematopoiesis in mice heterozygous for an AML1-ETO fusion gene. Nat Genet. 1997;15:303-306.

33. Okuda T, Cai Z, Yang S, et al. Expression of a knocked-in AML1-ETO leukemia gene inhibits the establishment of normal definitive hematopoiesis and directly generates dysplastic hematopoietic progenitors. Blood. 1998;91:3134-3143.

34. Yagi T, Tokunaga T, Furuta Y, et al. A novel ES cell line, TT2, with high germline-differentiating potency. Anal Biochem. 1993;214:70-76.

35. Ashihara E, Vannucchi AM, Migliaccio G, Migliaccio AR. Growth factor receptor expression during in vitro differentiation of partially purified populations containing murine stem cells. J Cell Physiol. 1997;171:343-356.

36. Kumano K, Chiba S, Shimizu K, et al. Notch1 inhibits differentiation of hematopoietic cells by sustaining GATA-2 expression. Blood. 2001;98:3283-3289.

37. Lecuyer E, Herblot S, Saint-Denis M, et al. The SCL complex regulates c-kit expression in hematopoietic cells through functional interaction with Sp1. Blood. 2002;100:2430-2440.

38. Harigae H, Nakajima O, Suwabe N, et al. Aberrant iron accumulation and oxidized status of erythroid-specific δ-aminolevulinate synthase (ALAS2)–deficient definitive erythroblasts. Blood. 2003;101:1188-1193.

39. Welch JJ, Watts JA, Vakoc CR, et al. Global regulation of erythroid gene expression by transcription factor GATA-1. Blood. 2004;104:3136-3147.

40. Lerga A, Crespo P, Berciano M, et al. Regulation of c-Myc and Max in megakaryocytic and monocytic-macrophagic differentiation of K562 cells induced by protein kinase C modifiers: c-Myc is down-regulated but does not inhibit differentiation. Cell Growth Differ. 1999;10:639-654.

41. Dahl R, Simon MC. The importance of PU.1 concentration in hematopoietic lineage commitment and maturation. Blood Cells Mol Dis. 2003;31: 229-233.

42. Okada H, Watanabe T, Niki M, et al. AML1(−/−) embryos do not express certain hematopoiesis-related gene transcripts including those of the PU.1 gene. Oncogene. 1998;17:2287-2293.

43. Friedman AD, Keefer JR, Kummalue T, Liu H, Wang QF, Cleaves R. Regulation of granulocyte and monocyte differentiation by CCAAT/enhancer binding protein α. Blood Cells Mol Dis. 2003;31: 338-341.

44. Warren AJ, Colledge WH, Carlton MB, Evans MJ, Smith AJ, Rabbitts TH. The oncogenic cysteine-rich LIM domain protein rbtn2 is essential for erythroid development. Cell. 1994;78:45-57.

45. Shivdasani RA, Mayer EL, Orkin SH. Absence of blood formation in mice lacking the T-cell leukaemia oncoprotein tal-1/SCL. Nature. 1995;373: 432-434.

46. Zhang P, Zhang X, Iwama A, et al. PU.1 inhibits GATA-1 function and erythroid differentiation by blocking GATA-1 DNA binding. Blood. 2000;96: 2641-2648.

47. Kreider BL, Orkin SH, Ihle JN. Loss of erythropoietin responsiveness in erythroid progenitors due to expression of the Evi-1 myeloid-transforming gene. Proc Natl Acad Sci U S A. 1993;90:6454-6458.

48. Louz D, van den Broek M, Verbakel S, et al. Erythroid defects and increased retrovirally-induced tumor formation in Evi1 transgenic mice. Leukemia. 2000;14:1876-1884.

49. Morishita K, Parganas E, Matsugi T, Ihle JN. Expression of the Evi-1 zinc finger gene in 32Dc13 myeloid cells blocks granulocytic differentiation in response to granulocyte colony-stimulating factor. Mol Cell Biol. 1992;12:183-189.

50. Scott EW, Simon MC, Anastasi J, Singh H. Requirement of transcription factor PU.1 in the development of multiple hematopoietic lineages. Science. 1994;265:1573-1577.

51. McKercher SR, Torbett BE, Anderson KL, et al. Targeted disruption of the PU.1 gene results in multiple hematopoietic abnormalities. EMBO J. 1996;15:5647-5658.

52. Anderson KL, Smith KA, Conners K, McKercher SR, Maki RA, Torbett BE. Myeloid development is selectively disrupted in PU.1 null mice. Blood. 1998;91:3702-3710.

53. DeKoter RP, Singh H. Regulation of B lymphocyte and macrophage development by graded expression of PU.1. Science. 2000;288:1439-1441.

54. McIvor Z, Hein S, Fiegler H, et al. Transient expression of PU.1 commits multipotent progenitors to a myeloid fate whereas continued expression favors macrophage over granulocyte differentiation. Exp Hematol. 2003;31:39-47.

55. Kim HG, De Guzman CG, Swindle CS, et al. The ETS family transcription factor, PU.1, is necessary for the maintenance of fetal liver hematopoietic stem cells. Blood. 2004;104:3894-3900.

56. Zhang DE, Zhang P, Wang ND, Hetherington CJ, Darlington GJ, Tenen DG. Absence of granulocyte colony-stimulating factor signaling and neutrophil development in CCAAT enhancer binding protein α-deficient mice. Proc Natl Acad Sci U S A. 1997;94:569-574.

57. Bockamp EO, McLaughlin F, Murrell AM, et al. Lineage-restricted regulation of the murine SCL/TAL-1 promoter. Blood. 1995;86:1502-1514.

58. Crable SC, Anderson KP. A PAR domain transcription factor is involved in the expression from a hematopoietic-specific promoter for the human LMO2 gene. Blood. 2003;101:4757-4764.

59. Rhoades KL, Hetherington CJ, Harakawa N, et al. Analysis of the role of AML1-ETO in leukemogenesis, using an inducible transgenic mouse model. Blood. 2000;96:2108-2115.

60. Higuchi M, O'Brien D, Kumaravelu P, Lenny N, Yeoh EJ, Downing JR. Expression of a conditional AML1-ETO oncogene bypasses embryonic lethality and establishes a murine model of human t(8;21) acute myeloid leukemia. Cancer Cell. 2002;1:63-74.

61. Yuan Y, Zhou L, Miyamoto T, et al. AML1-ETO expression is directly involved in the development of acute myeloid leukemia in the presence of additional mutations. Proc Natl Acad Sci U S A. 2001;98:10398-10403.

Clinical characteristics and prognostic implications of *NPM1* mutations in acute myeloid leukemia

Tatsuya Suzuki, Hitoshi Kiyoi, Kazutaka Ozeki, Akihiro Tomita, Satomi Yamaji, Ritsuro Suzuki, Yoshihisa Kodera, Shuichi Miyawaki, Norio Asou, Kazutaka Kuriyama, Fumiharu Yagasaki, Chihiro Shimazaki, Hideki Akiyama, Miki Nishimura, Toshiko Motoji, Katsuji Shinagawa, Akihiro Takeshita, Ryuzo Ueda, Tomohiro Kinoshita, Nobuhiko Emi, and Tomoki Naoe

Recently, somatic mutations of the nucleophosmin gene *(NPM1)*, which alter the subcellular localization of the product, have been reported in acute myeloid leukemia (AML). We analyzed the clinical significance of *NPM1* mutations in comparison with cytogenetics, *FLT3*, *NRAS*, and *TP53* mutations, and a partial tandem duplication of the *MLL* gene (MLL-TD) in 257 patients with AML. We found *NPM1* mutations, including 4 novel sequence variants, in 64 of 257 (24.9%) patients. *NPM1* mutations were associated with normal karyotype and with internal tandem duplication (ITD) and D835 mutations in *FLT3*, but not with other mutations. In 190 patients without the M3 French-American-British (FAB) subtype who were treated with the protocol of the Japan Adult Leukemia Study Group, multivariate analyses showed that the *NPM1* mutation was a favorable factor for achieving complete remission but was associated with a high relapse rate. Sequential analysis using 39 paired samples obtained at diagnosis and relapse showed that *NPM1* mutations were lost at relapse in 2 of the 17 patients who had *NPM1* mutations at diagnosis. These results suggest that the *NPM1* mutation is not necessarily an early event during leukemogenesis or that leukemia clones with *NPM1* mutations are sensitive to chemotherapy. (Blood. 2005;106:2854-2861)

© 2005 by The American Society of Hematology

Introduction

Acute myeloid leukemia (AML) is characterized by autonomous proliferation and impaired differentiation of hematopoietic progenitors but is a genetically and phenotypically heterogeneous disease. A number of genetic mutations, such as point mutations, gene rearrangements, and chromosomal translocations, which are involved in the pathogenesis of leukemia, have been documented. Recently, it was suggested that AML is the consequence of 2 broad complementation classes of mutations: those that confer a proliferative or a survival advantage to hematopoietic progenitors (class 1) —including activating mutations in tyrosine kinases such as *BCR-ABL1*, *ETV6-PDGFRB*, *KIT*, and *FLT3* or their downstream effectors such as *NRAS*—and those that impair hematopoietic differentiation and confer properties of self-renewal (class 2)— including rearrangements or point mutations of core binding factor *(CBF)* genes and *PML-RARA*.[1] Mutations in *FLT3*, *NRAS*, and *KIT* have been found in approximately 30% to 35%, 15% to 20%, and

5% to 10% of adult patients with AML, respectively, indicating that mutations in these 3 genes are the most frequent genetic alterations in AML.[2-12] *FLT3* and *KIT* mutations are often found in AML patients with *PML-RARA* and *CBF* gene translocations, respectively,[13,14] whereas *FLT3* mutations have been preferentially found in AML patients with normal karyotype. Because mutated FLT3 reportedly induces myeloproliferative disease (MPD), but not AML, in primary hematopoietic progenitors in the murine bone marrow transplantation model and MPD does not have serial transplantability, *FLT3* mutations alone are not sufficient for the development of AML.[15] Therefore, it has been suggested that additional mutations are involved in the pathogenesis of AML with *FLT3* mutations.

Recently, Falini et al[16] reported that the nucleophosmin gene *(NPM1)* is mutated in a high proportion of adults with AML, resulting in an aberrant cytoplasmic localization of the product

(NPMc+). Of note is that NPMc+ is associated with a wide spectrum of morphologic subtypes of AML, a normal karyotype, and FLT3 mutations. Furthermore, NPMc+ AML is clinically associated with better responsiveness to induction chemotherapy, although its prognostic implications for long-term outcome remain unclear. Although the prevalence and significance of several genetic abnormalities in patients with AML have been reported to date, the most powerful prognostic factor in AML has been the karyotype of the leukemia cells.[17] Three cytogenetic risk groups (favorable, intermediate, and poor) are widely accepted, but there is a practical limitation to the definition of cytogenetic risk, especially in patients in the intermediate group. Additional prognostic factors are, therefore, required. We and several groups[9,10,12,18] have demonstrated that FLT3 mutations are a strong prognostic factor in AML, especially in patients with normal karyotype, but they do not affect responsiveness to induction chemotherapy. Therefore, NPM1 mutations seem to characterize a distinct disease entity not only of AML with normal karyotype but also of AML with FLT3 mutations.

NPM is a ubiquitously expressed phosphoprotein, continuously shuttles between the nucleus and the cytoplasm,[19,20] and is involved in the oncogenesis of some types of leukemia and lymphoma because the NPM gene is a partner in several tumor-associated chromosomal translocations.[21-23] However, it is also thought to have a tumor-suppressor function and to regulate the p53 pathway through its chaperoning activity.[24-26] It is suggested that a loss of nuclear NPM function caused by mutation might impair the p53 pathway and that a lack of p53 might induce genetic instability[27]; hence, NPM1 mutations seem to cause AML cells to acquire additional genetic alterations.

In this study, we analyzed the prevalence and clinical characteristics of NPM1 mutations in comparison with cytogenetics, FLT3, NRAS, and TP53 mutations and a partial tandem duplication of the MLL gene (MLL-TD) in 257 patients with newly diagnosed de novo AML. The prognostic implications of NPM1 mutations were evaluated in 190 patients with AML, excluding those with the M3 FAB subtype, who were treated according to the protocol of the Japan Adult Leukemia Study Group (JALSG). Furthermore, to clarify the stability of NPM1 mutations and the potential effect on genetic instability in AML cells during disease progression, we compared the mutational status of these genes in 39 paired samples obtained at initial diagnosis and first relapse.

Patients, materials, and methods

Patients and samples

The diagnosis of AML was based on the French-American-British (FAB) classification. The study population included 257 patients with newly diagnosed de novo AML, as follows: 9 with the M0, 54 with the M1, 89 with the M2, 15 with the M3, 54 with the M4, 19 with the M5, 8 with the M6, and 9 with the M7 FAB subtype. In 39 of the 257 AML patients, paired samples obtained at diagnosis and first relapse were available. Furthermore, in 6 patients, samples obtained at diagnosis and complete remission (CR) were available. Bone marrow (BM) samples from patients with AML were subjected to Ficoll-Hypaque (Pharmacia LKB, Uppsala, Sweden) density gradient centrifugation. All samples taken at diagnosis or relapse were confirmed to contain more than 90% leukemia cells after enrichment by centrifugation. Informed consent was obtained from all patients to use their samples for banking and molecular analysis, and approval for these studies was obtained from the Nagoya University institutional review board.

Cytogenetic G-banding analysis was performed according to standard methods. In this study, cytogenetic risk groups were stratified according to the criteria adopted by the Medical Research Council.[28]

Screening for mutations of the FLT3, NRAS, and TP53 genes and of MLL-TD

High molecular weight DNA and total RNA were extracted from the samples using standard methods. FLT3 gene mutations of the ITD (FLT3/ITD) and activation loop (FLT3/D835Mt), NRAS gene mutations of codons 12, 13, and 61, and TP53 gene mutations of exons 5 to 8 were examined as reported and were confirmed by the sequencing procedure.[4,29,30] MLL-TD was examined by reverse transcription–polymerase chain reaction (RT-PCR), as described previously.[31]

Screening for mutations of the NPM1 gene

For the screening of NPM1 mutations, we amplified genomic DNA corresponding to exon 12 of NPM1 by PCR using the primers NPM1-F, 5'-TTAACTCTCTGGTGGTAGAATGAA-3' and NPM1-R, 5'-CAAGAC-TATTTGCCATTCCTAAC-3', as previously reported.[16] Amplified products were separated through agarose gel, purified using a QIAquick gel extraction kit (Qiagen Inc, Chatsworth, CA), and directly sequenced on a DNA sequencer (310; Applied Biosystems, Foster City, CA) using a BigDye terminator cycle sequencing kit (Applied Biosystems). If mutations were found by direct sequencing, the fragments were cloned into a pGEM-T Easy vector (Promega, Madison, WI), then transfected into the Escherichia coli strain DH5α. At least 4 recombinant colonies were selected, and plasmid DNA was prepared using a QIAprep Spin Miniprep Kit (Qiagen Inc) and sequenced.

Analysis of clinical characteristics

It was necessary to analyze the clinical characteristics in a well-documented group. Among the 257 patients analyzed, 15 had acute promyelocytic leukemia (APL). APL has been considered a separate disease entity among AML, and the introduction of all-trans retinoic acid (ATRA) has dramatically improved its clinical outcome.[32] In addition, 52 patients with AML, excluding those with APL, were treated with independent regimens. We, therefore, analyzed the clinical characteristics of 190 patients with AML, excluding those with APL, who were treated with the AML87, AML89, and AML92 protocols of JALSG.[33-35] (Each protocol is presented in Document S1; see the Supplemental Document link at the top of the online article, at the Blood website.)

Statistical analysis

Differences in continuous variables were analyzed using the Mann-Whitney U test for distribution between 2 groups. Analysis of frequencies was performed using the Fisher exact test for 2 × 2 tables or the Pearson χ^2 test for larger tables. Multivariate analysis to identify risk factors for achieving CR was performed using the logistic regression model. Survival probabilities were estimated by the Kaplan-Meier method, and differences in survival distributions were evaluated using the log-rank test. Overall survival was defined as the time from the first day of therapy to death or last visit. Relapse-free survival was defined as the time from the first day of CR to relapse, death, or last visit. Patients undergoing hematopoietic stem cell transplantation were censored at the time of transplantation. The prognostic significance of the clinical variables was assessed using the Cox proportional hazards model. These statistical analyses were performed with StatView-J 5.0 (Abacus Concepts Inc, Berkeley, CA). For all analyses, the P values were 2-tailed, and $P < .05$ was considered statistically significant.

Results

NPM1 mutations were frequently found in AML

We first screened for mutations within exon 12 of the NPM1 gene through direct sequencing in 257 patients with AML, then confirmed

each type of mutation by cloning. We found the *NPM1* mutation in 64 of 257 (24.9%) patients (Table 1). Importantly, direct sequencing revealed that all AML cells with *NPM1* mutations retained the wild-type allele. Given that all samples contained more than 90% AML cells, all mutations seemed to occur in only one allele. Previously, 6 kinds of mutants, designated mutations A to F, were identified. In this study, we found 49 mutations of type A, 7 mutations of type B, 4 mutations of type D, and 4 novel mutants that were designated mutations G to J (Figure 1). All novel mutations included distinct 4-bp insertions (mutation G, TTTG; mutation H, CTTG; mutation I, TAAG; mutation J, TATG) at position 960, resulting in the same frameshift as mutations A to D. Predicted mutant proteins of mutations G and H and of mutation J were the same as those of mutations A and B, respectively. The protein of mutation I contained a lysine residue at position 289, although the other residues were conserved.

Table 1. Relationship among *NPM1* mutation, FAB type, and genetic alterations in AML

	Total no. patients	*NPM1* Mutation, no. (%)*	*NPM1* Wild type, no. (%)†	P
FAB subtype				.005
M0	9	2 (22.2)	7 (77.8)	
M1	54	17 (31.5)	37 (68.5)	
M2	89	12 (13.5)	77 (86.5)	
M3	15	0 (0)	15 (100)	
M4	54	21 (38.9)	33 (61.1)	
M5	19	9 (47.3)	10 (52.7)	
M6	8	2 (25.0)	6 (75.0)	
M7	9	1 (11.1)	8 (88.9)	
Cytogenetics				< .001
t(8;21)	31	0 (0)	31 (100)	
inv(16)	8	1 (12.5)	7 (87.5)	
t(15;17)	15	0 (0)	15 (100)	
t(9;22)	3	1 (33.3)	2 (66.7)	
del(5)	7	0 (0)	7 (100)	
del(7)	5	0 (0)	5 (100)	
Others	43	5 (11.6)	38 (88.4)	
Normal	97	46 (47.4)	51 (52.6)	
Unknown	48	11 (22.9)	37 (77.1)	
FLT3				
Mutations, total	67	39 (58.2)	28 (41.8)	< .001
ITD	58	35 (60.3)	23 (39.7)	< .001‡
D835	9	4 (44.4)	5 (55.6)	.028‡
Wild type	190	25 (13.2)	165 (86.8)	
TP53				NS
Mutation	16	2 (12.5)	14 (87.5)	
Wild type	227	58 (25.6)	169 (74.4)	
Not done	14	5 (35.7)	10 (64.3)	
NRAS				NS
Mutation	34	9 (26.5)	25 (73.5)	
Wild type	202	48 (23.8)	154 (76.2)	
Not done	21	7 (33.3)	14 (66.7)	
MLL-TD				NS
Mutation	17	2 (11.8)	15 (88.2)	
Wild type	130	33 (25.4)	97 (74.6)	
Not done	110	29 (26.4)	81 (73.6)	

Numbers and percentages of 257 patients with AML are shown by FAB type; cytogenetics; and *FLT3*, *TP53*, *NRAS*, and MLL-TD mutations, according to *NPM1* mutation.

NS indicates not significant.

*n = 64; 24.9%.

†n = 193; 75.1%.

‡These variables were compared with those of the wild type.

In 2 patients whose leukemia cells had *NPM1* mutations at diagnosis, the mutations were lost at CR, indicating that these were somatic mutations.

Morphologic and genotypic characteristics of AML with *NPM1* mutations

NPM1 mutations were found in patients with AML of all FAB subtypes except M3 (Table 1). Cytogenetic data were available for 209 patients. Consistent with findings of a previous report,[16] the *NPM1* mutation was preferentially found in patients with normal karyotype (46 of 97; 47.4%), but it was not found in patients with t(8;21), t(15;17), del(5), or del(7). In total, there was a significant difference in the frequency of the *NPM1* mutation among patients with (7 of 112; 6.3%) and without (46 of 97; 47.4%) cytogenetic abnormalities (P < .001). Moreover, an *NPM1* mutation was found in each of 8 and 3 patients with inv(16) and t(9;22), respectively.
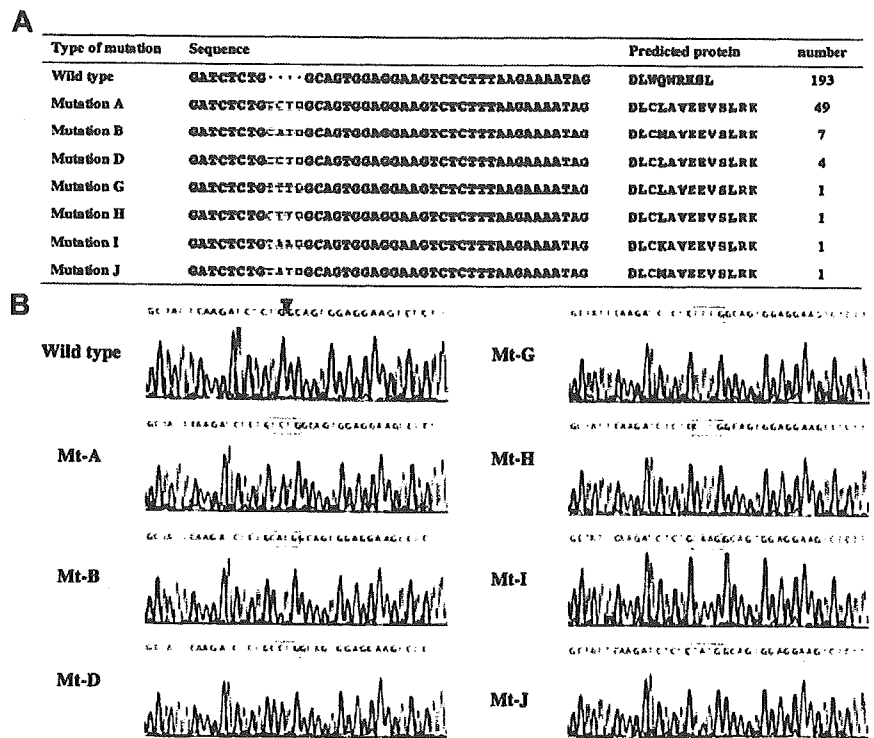
FLT3/ITD and FLT3/D835Mt were found in 58 (22.6%) and 9 (3.5%) of 257 patients, respectively (Table 1). Both *FLT3* mutations were significantly associated with *NPM1* mutations: 35 of 58 (60.3%) FLT3/ITD (P < .001) and 4 of 9 (44.4%) FLT3/D835Mt (P = .028) were found in the patients with *NPM1* mutations. *TP53*, *NRAS*, and MLL-TD mutations were found in 16 of 243 (6.6%), 34 of 236 (14.4%), and 17 of 147 (11.6%) patients, respectively, although there was no significant correlation between these mutations and the *NPM1* mutation (Table 1).

Clinical characteristics and prognoses of AML patients with or without *NPM1* mutations

Among the 257 patients with AML, 190 patients (excluding those with M3 who were treated with the AML87, AML89, and AML92 protocols of the JALSG) were evaluated for clinical characteristics and initial response to therapy (Table 2). Of these patients, 49 (25.8%) had *NPM1* mutations. The presence of *NPM1* mutations was related neither to sex nor to the occurrence of hepatosplenomegaly or extramedullary involvement. Patients with *NPM1* mutations (median, 58 years; range, 15-77 years) were significantly older than those without mutations (median, 47 years; range, 15-85 years) (P = .003). White blood cell (WBC) counts and peripheral blood blast cells were significantly higher in the *NPM1* mutation group than in the wild-type group (P = .002 and P = .029, respectively). According to the FAB classification, the *NPM1* mutation was infrequent in the M2 subtype (P = .004). According to the cytogenetic risk groups, the *NPM1* mutation was preferentially found in the intermediate risk group (P < .001). *NPM1* mutations were associated with FLT3/ITD (P < .001) and FLT3/D835Mt (P = .018), but not with *TP53* and *NRAS* mutations. Because we could analyze MLL-TD in only 118 of the 190 patients, we excluded MLL-TD from the variables for statistical analysis.

Of the 190 patients, 139 (73.2%) achieved CR after induction chemotherapy. The CR rate was significantly higher in the patients with *NPM1* mutations (42 of 49; 85.7%) than without them (97 of 141; 68.8%) (P = .025). In addition, Fisher exact test showed that FAB subtypes other than M2, cytogenetic findings other than good risk, and the presence of *NRAS* and *TP53* mutations were unfavorable factors for achieving CR (P < .001, P = .002, P = .030, and P = .034, respectively). Age (older than 60), WBC count (more than 100 × 10^9/L), and presence of the *FLT3* mutation were not associated with the CR rate. Multivariate logistic regression analysis showed that wild-type *NPM1* (P < .001), FAB subtypes other than M2 (P = .008), and cytogenetic findings other than good

Figure 1. Mutations in NPM1 exon 12. (A) The mutated nucleotide and the predicted amino acid sequence in *NPM1* exon 12 found in the present study are shown in comparison with the wild-type sequence. Type of mutation (mutations A, B, D) is designated according to a previous report. Four novel mutant variants are designated mutations G, H, I, and J. Red and blue indicate nucleotide insertions and termination codons, respectively. Green indicates the conserved residues in mutant NPM. Purple indicates putative residues of a consensus nuclear export signal (Lx[1-3]Vx[2-3]VxL; x indicates any residue). (B) Sequence results after cloning. Boxes indicate inserted 4-bp nucleotides. Arrowhead indicates the position of the insert at nucleotide 960 of the *NPM1* gene.

A

Type of mutation	Sequence	Predicted protein	number
Wild type	GATCTCTG···GCAGTGGAGGAAGTCTCTTTAAGAAAATAG	DLWQNRRSL	193
Mutation A	GATCTCTGTCTGGCAGTGGAGGAAGTCTCTTTAAGAAAATAG	DLCLAVEEVSLRK	49
Mutation B	GATCTCTGCATGGCAGTGGAGGAAGTCTCTTTAAGAAAATAG	DLCMAVEEVSLRK	7
Mutation D	GATCTCTGCCTGGCAGTGGAGGAAGTCTCTTTAAGAAAATAG	DLCLAVEEVSLRK	4
Mutation G	GATCTCTGTTTGGCAGTGGAGGAAGTCTCTTTAAGAAAATAG	DLCLAVEEVSLRK	1
Mutation H	GATCTCTGCTTGGCAGTGGAGGAAGTCTCTTTAAGAAAATAG	DLCLAVEEVSLRK	1
Mutation I	GATCTCTGTAAGGCAGTGGAGGAAGTCTCTTTAAGAAAATAG	DLCKAVEEVSLRK	1
Mutation J	GATCTCTGCATGGCAGTGGAGGAAGTCTCTTTAAGAAAATAG	DLCMAVEEVSLRK	1

B

risk (*P* = .039) were independent unfavorable factors for achieving CR (Table 3).

Kaplan-Meier analyses according to *NPM1* mutation are shown in Figure 2A. Univariate analysis showed that the poor prognostic factors for overall survival were age 60 or older (*P* = .001), mutation of *TP53* (*P* < .001), FAB subtypes other than M2 (*P* = .005), FLT3/ITD (*P* = .010), high WBC count (more than 100×10^9/L) (*P* = .019), and cytogenetic findings (poor vs others) (*P* = .024). Multivariate Cox regression analysis with stepwise selection showed that the mutation of *TP53* (odds ratio, 4.002 [95% confidence interval (CI), 1.876-8.538]; *P* < .001), age 60 or older (odds ratio, 1.651 [95% CI, 1.131-2.410]; *P* = .009), and FAB subtypes other than M2 (odds ratio, 1.643 [95% CI, 1.127-2.396]; *P* = .010) were independent poor prognostic factors for overall survival (Table 4). When adjusted with age 60 years or older, FLT3/ITD, FAB subtype other than M2, high WBC count (more than 100×10^9/L), and mutation of *NRAS*, mutation of *NPM1* was an adverse prognostic factor (odds ratio, 1.949 [95% CI, 1.164-3.268]; *P* = .011). Although careful assessment and further investigation are needed, the mutation of *NPM1* may act as a prognostic factor for overall survival.

Because only 1 of 139 patients who achieved CR died during CR, we compared the probability of relapse between patients with and without *NPM1* mutations (Figure 2A). Univariate analysis showed that the unfavorable factors for relapse were mutation of *NPM1* (*P* = .006), FLT3/ITD (*P* = .007), cytogenetic findings (poor vs others) (*P* = .007), high WBC count (more than 100×10^9/L) (*P* = .016), FAB subtypes other than M2 (*P* = .024), and age 60 or older (*P* = .024). Multivariate Cox regression analysis with stepwise selection identified that cytogenetic findings (poor vs others) (odds ratio, 3.876 [95% CI, 1.718-8.772]; *P* = .001) and mutation of *NPM1* (odds ratio, 2.106 [95% CI, 1.324-3.350]; *P* = .002) were independent unfavorable factors for relapse (Table 5).

In addition, we analyzed the prognostic value of *NPM1* mutations in 79 patients with normal karyotype. *NPM1* mutations were found in 37 of 79 (46.8%) patients. Of these 79 patients, 59

(74.7%) achieved CR after induction chemotherapy. The CR rate was significantly higher in the patients with *NPM1* mutations (32 of 37; 86.4%) than in those without (27 of 42; 64.3%) (*P* = .037 by Fisher exact test). Multivariate logistic regression analysis, including wild-type *NPM1*, FAB subtypes (other than M2), presence of *FLT3*, *NRAS*, and *TP53* mutations, age (older than 60 years), and WBC count (more than 100×10^9/L) showed that wild-type *NPM1* was the only independent unfavorable factor for achieving CR (odds ratio, 4.908 [95% CI, 1.011-23.824]; *P* = .048). Kaplan-Meier curves according to *NPM1* mutation in this group are shown in Figure 2B. Multivariate Cox regression analysis with stepwise selection showed that age 60 or older was the only poor prognostic factor for overall survival (odds ratio, 2.068 [95% CI, 1.175-3.641]; *P* = .012). Mutation of *NPM1* was not a significant prognostic factor for overall survival regardless of whatever factors were used for adjustment by means of Cox analysis. The relapse risk was analyzed in 59 patients who achieved CR. Multivariate Cox regression analysis with stepwise selection identified that the *NPM1* mutation was the only independent unfavorable factor for relapse (odds ratio, 2.096 [95% CI, 1.050-4.186]; *P* = .036). However, because the patient number of this group was small, larger-scale analysis was required.

FLT3/ITD has been identified as an unfavorable prognostic factor in patients with AML, although the prognostic implications of FLT3/D835Mt remain unclear. Given that the *NPM1* mutation was associated with FLT3/ITD, it was important to define the role of *NPM1* mutations alone or in combination with FLT3/ITD for long-term prognosis. Therefore, we compared the clinical impact of *NPM1* mutations in patients with and without FLT3/ITD. Interestingly, mutation of *NPM1* was an independent favorable prognostic factor for CR in patients with FLT3/ITD (odds ratio, 20.8 [95% CI, 2.0-200]; *P* = .011 by multivariate logistic regression analysis), but it did not affect the CR rate in patients without FLT3/ITD. In addition, mutation of *NPM1* was a favorable prognostic factor for overall survival in patients with FLT3/ITD (*P* = .045), but not in those without FLT3/ITD. However, mutation